APPENDIX C

RELIABILITY ANALYSIS OF THREE-SPAN BRIDGE MODEL

1. TRADITIONAL SCOUR EVALUATION APPROACH

The AASHTO LRFD specifications (1994) state that "a majority of bridges that have failed in the United States and elsewhere have failed due to scour." This is confirmed by Shirole and Holt (1991), who observed that over the last 30 years, more than 1,000 of the 600,000 U.S. bridges have failed and that 60% of these failures are due to scour while earthquakes accounted for only 2%. Of course, there are many more bridges that are posted or otherwise taken out of service due to their inadequate strengths (e.g., due to deterioration, low rating, fatigue damage, etc.); nevertheless, scour is considered a critical cause of failure because its occurrence often leads to total collapse. For these reasons, developing methods for the design and maintenance of bridge foundations for scour is currently considered a top priority for agencies concerned with the safety of bridges.

The AASHTO LRFD specifications require that scour at bridge foundations be designed for the 100-year flood storm surge tide or for the overtopping flood of lesser recurrence interval. The corresponding 100-year design scour depth at bridge foundations is determined following the procedure recommended by FHWA, using what is known as "HEC-18" (Hydraulic Engineering Circular No. 18 [Richardson and Davis, 1995]). The foundation should then be designed taken into consideration the design scour depth. This is achieved by, for example, placing the footings below the scour depth, ensuring that the lengths of piles and pile shafts extend beyond the scour depth, and verifying that the remaining soil depth after scour provide sufficient resistances against shear failures and overturning.

HEC-18 recognizes that the total scour at a highway crossing is comprised of three components:

1. Long-term aggradation and degradation,
2. Contraction scour, and
3. Local scour.

Aggradation and degradation are long-term elevation changes in the streambed of the river or waterway caused by erosion and deposition of material. Contraction scour is due to the removal of material from the bed and the banks of a channel, often caused by the bridge embankments encroaching onto the main channel.

Local scour involves the removal of material from around bridge piers and abutments. It is caused by an acceleration of flow around the bridge foundation that accompanies a rise in water levels that may be due to floods and other events. Local scour and contraction scour can be either clear-water or live-bed. Live-bed conditions occur when there is a transport of bed material in the approach reach. Clear-water conditions occur when there is no bed material transport. Live-bed local scour is cyclic in nature as it allows the scour hole that develops during the rising stage of the water flow to refill during the falling stage. Clear-water scour is permanent because it does not allow for a refill of the hole.

In this research effort, attention was focused on local live-bed scour around bridge piers that, because of its cyclical nature, is the most unpredictable type of scour. For local scour around bridge piers, HEC-18 recommends the use of the following design equation to predict the 100-year design scour depth:

$$y_{\max} = 2y_0K_1K_2K_3K_4\left(\frac{D}{y_0}\right)^{0.65}F_0^{0.43} \quad (1)$$

where

$y_{\max}$ = the maximum depth of scour;
Y_0 = the depth of flow just upstream of the bridge pier excluding local scour;
K_1, K_2, K_3 and K_4 = coefficients that account for the nose shape of the pier, the angle between the direction of the flow and the direction of the pier, the streambed conditions, and the bed material size;
D = the pier diameter, and
F_0 = the Froude number defined as follows:

$$F_0 = \frac{V}{(gy_0)^{0.5}} \quad (2)$$

where V is the mean flow velocity at the pier, and g is the acceleration due to gravity.

The process that is followed to calculate the 100-year design (or nominal) scour depth for a bridge pier is as follows:

1. Use statistical data on flood events for the bridge site to obtain the expected maximum 100-year flood discharge rate.
2. Perform a hydraulic analysis to obtain the corresponding expected maximum 100-year flow velocity, V, and the 100-year stream flow depth, y_0.
3. Use the information from Step 2 to calculate the Froude number.

4. Use information on pier geometry, streambed conditions and angle of attack, and streambed material to calculate D, K_1, K_2, K_3 and K_4.
5. Substitute the values obtained into the HEC-18 Equation 1 to calculate the 100-year design scour depth for the bridge under consideration.

The objective of this project, NCHRP Project 12-48, is to calibrate load factors for the scour extreme event and the combination of scour with other extreme events such as earthquakes, winds, and ship collisions. The calibration should be performed using reliability methods to be compatible with the AASHTO LRFD specifications. The calibration process requires the evaluation of the reliability inherent in current design practice. The steps of the calibration process involve

1. "Designing" a number of typical bridges to satisfy current specifications.
2. Finding the inherent reliability in these designs.
3. Finally, calibrating a set of load factors to ensure that bridges designed with these factors will satisfy a target reliability that will be determined based on the experience gained from previous designs.

This appendix focuses on developing a model for calibrating load factors for bridges subjected to the combination of scour and earthquake forces. Current design practice for scour uses the HEC-18 equations published by FHWA. This section illustrates the use of HEC-18 for finding the scour depth at a bridge pier. The methods will subsequently be used to develop a model to study the reliability of bridges subjected to scour and a model to study the reliability of bridges subjected to the combined effects of scour and earthquake forces.

1.1 Illustrative Example

To illustrate the use of the HEC-18 equation to find the scour depth at a bridge pier, we assume that we are to design a bridge for the 100-year scour. The bridge is to be located over a 220-ft wide segment of a river, and the bridge will have the configuration shown in Figure 1.

The bridge is constructed over a 200-ft wide river. To obtain realistic results for different possible discharge rates, data from different small size rivers are used and design scour depths are calculated for each of these river discharge rates. The rivers chosen for this analysis consist of the following: (1) Schohaire Creek in upstate New York, (2) Mohawk River in upstate New York, (3) Cuyahoga River in northern Ohio, (4) Rocky River in Ohio, and (5) Sandusky River in Ohio. Data on the peak annual discharge rates for each of the five rivers was obtained from the U.S. Geological Survey (USGS) website. Lognormal probability plots and Kolmogorov–Smirnov (K-S) goodness-of-fit tests showed that the peak annual discharge rate, Q, for all five rivers can be well modeled by lognormal probability distributions. The mean of the log Q and its standard deviation were calculated using a maximum likelihood estimator. This data are provided in Table 1, along with the K-S maximum difference in cumulative distribution, Dn. D_n^* is the K-S maximum difference between the measured cumulative probability and expected probability value. More than 60 data points were available for each of the five rivers. This indicates

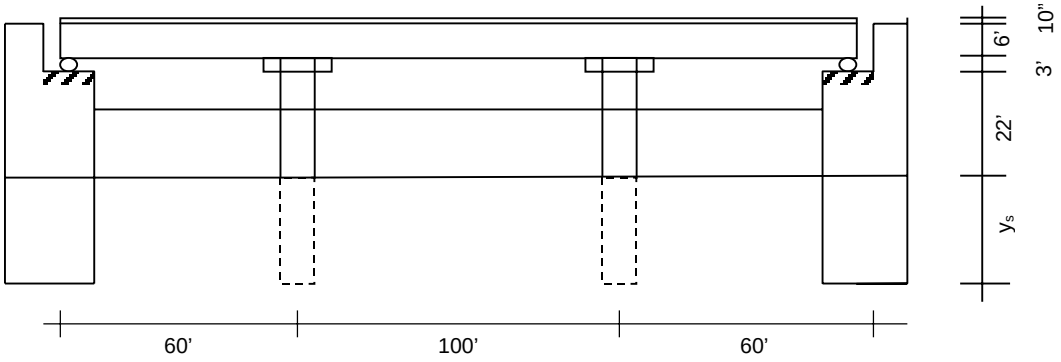

Figure 1. Profile of example bridge.

TABLE 1 Probability models for five rivers

River	Log Q	$S_{\log Q}$	D_n^*
Schohaire	9.925	0.578	0.067
Mohawk	9.832	0.243	0.068
Sandusky	9.631	0.372	0.086
Cuyahoga	9.108	0.328	0.065
Rocky	9.012	0.378	0.049

that the lognormal distribution is acceptable for a significant levels $\alpha = 20$ percent.

In this example, we will assume that the width of the channel at the bridge site is permanently set at 220 ft, as shown in Figure 1. The rate of flow, Q, at a given point in time is related to the cross sectional area of the stream, A_0, and the stream flow velocity, V, by

$$Q = A_0 V. \tag{3}$$

For a rectangular cross section with a constant width, b, and flow depth, Y_0, the relationship becomes

$$Q = by_0 V. \tag{4}$$

The flow velocity, V, depends on the flow depth, y_0. The relationship between the flow velocity, V, and flow depth, y_0, can be expressed using Manning's equation:

$$V = \frac{\Phi}{n} R^{2/3} S^{1/2} \tag{5}$$

where

n = the Manning roughness coefficient, which would vary between 0.025 to 0.035 for earth (respectively for good condition and for weeds and stones);
R = the hydraulic radius;
S = the slope of the bed stream; and
Φ = an empirical factor equal to 1.486 when using U.S. units (ft and sec).

For SI units, F = 1.0. For the problem described in Figure 1, the hydraulic radius, R, can be calculated by

$$R = \frac{by_0}{2 + y_0}. \tag{6}$$

In this illustration, we will assume a slope of $S = 0.2\%$. Using the equations given above, the relationship between the flow rate Q and the flow depth y is given from the equation

$$Q = by_0 \frac{\Phi}{n} \left(\frac{by_0}{b + 2y_0} \right)^{2/3} S^{1/2} \tag{7}$$

where the following is input data:

$b = 220$ ft,
$\Phi = 1.486$,
$n = 0.025$, and
$S = 0.2\%$.

For the discharge rate data for each river shown in Table 1, the flow depth for the 100-year flood can be calculated as y_0 along with the corresponding velocity v. Given this information and the geometric data of the river and the bridge pier, the maximum design scour depth can be calculated from Equation 1. In this example, it is assumed that the round nose pier is aligned with the flow and that the bed material is sand. HEC-18 then recommends that the factors K_1, K_2, and K_4 all be set equal to 1.0. For plane bed condition, K_3 is equal to 1.1. Using Equation 1 with the column diameter of $D = 6$ ft, the design scour depth is obtained for each river as shown in Table 2.

1.2 Discussion

To study the safety of bridges accounting for the combined effect of scour and other extreme events, we need to know the extent of scour for different flood intensities, and we also need to know how the scour depth varies with time. This includes the time it takes for the flood to produce the maximum scour and the duration of the foundation exposure after the occurrence of scour before refill. Time becomes an important parameter because it controls the probability of having a simultaneous occurrence of scour and other events.

The HEC-18 approach has been used extensively for practical design considerations although the HEC-18 empirical model provides conservative estimates of scour depths and is known to have the following limitations:

1. The HEC-18 equation is based on model scale experiments in sand. In a recent evaluation against full-scale observations from 56 bridge sites, it was found to vastly over-predict the scour depth (Landers and Mueller, 1996). A comparison between the HEC-18 equation and the measured depths are illustrated in Figure 2, which is adapted from Landers and Mueller (1996).

TABLE 2 Design scour depth for each river

River	Q 100-year (ft^3/sec)	V (ft/sec)	Y_0-flood depth (ft)	Y_{max}-scour depth (ft)
Schohaire	78,146	17.81	20.56	17.34
Mohawk	32,747	12.87	11.78	13.99
Sandusky	36,103	13.35	12.52	14.33
Cuyahoga	19,299	10.5	8.45	12.26
Rocky	19,693	10.58	8.56	12.32

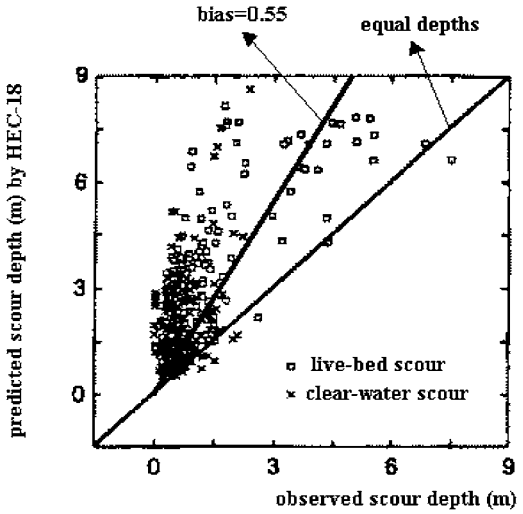

Figure 2. Comparison of HEC-18 predictions with observed scour depths.

2. Once a flood begins, it takes a certain amount of time for the full extent of erosion to take effect. Thus, if the flood is of a short duration, the maximum scour depth may not be reached before the flood recedes. On the other hand, prior floods may have caused partial erosions accelerating the attainment of the maximum scour depth. HEC-18 does not predict the length of time required for the maximum scour depth to be reached and assumes that the maximum depth is always reached independent of the flood duration and the level of scour incurred by prior floods.
3. The HEC-18 model does not distinguish between live-bed scour and clear-water scour in terms of the time required to reach equilibrium scour depth and the differences in the expected magnitudes of scour depths for these different phenomena (Richardson and Davis, 1995).
4. HEC-18 was developed based on experimental data obtained for sand materials. Some work is in progress to extend the use of HEC-18 for both sand and clay streambed materials although it is known that these materials behave differently (Briaud et al., 1999).
5. The usual assumption is that scour is deepest near the peak of a flood, but may be hardly visible after floodwaters recede and scour holes refill with sediment. However, there are no known methods to model how long it takes a river to back-fill the scour hole. Refill can occur only under live-bed conditions and depends on the type and size of the transported bed material (i.e., sand or clay). In any case, even if refill occurs, it will take a considerable time for the refill material to consolidate enough to restore the pier foundation to its initial strength capacity. Although such information is not precisely available, a number of bridge engineers have suggested that periods of 2 to 3 months are reasonable for clay materials with longer periods required for sands.
6. Based on the observations made above, it is evident that using the 100-year flow velocity and flow depth in the HEC-18 equations does not imply that the annual probability of failure will be 1/100. This is primarily due to the inherent conservative bias associated with the HEC-18 equation. In fact, based on observed scour depths at 515 sites, Johnson (1995) has shown that the HEC-18 equation produces scour depth estimates that are on the average 1.8 times higher than the measured values. This shows that the HEC-18 equation has a bias equal to 0.55 (1/1.8). The observed differences between predictions and measurements produced a coefficient of variation (COV; standard deviation/mean) of 52%. Figure 2 shows that these estimates are reasonable when compared with the data collected by Landers and Muller (1996).

Based on the observations made herein, an appropriate reliability model for the safety analysis of a bridge pier under the effect of scour is proposed, as illustrated in Section 2 of this report. This model is based on the work presented in Appendix B of the interim report for NCHRP Project 12-48.

2. RELIABILITY ANALYSIS FOR SCOUR

The HEC-18 model stipulates that previous levels of scour at the site do not affect the scour depth produced by a given flood. Hence, the maximum scour in a given return period is a function of the maximum flood observed in that period and is not affected by previous smaller floods that may have occurred within that same period. In addition, the HEC-18 model assumes that the flood duration is always long enough for the full scour depth corresponding to the flood velocity to be reached.

Although the scour hole is normally assumed to refill as the scour-causing flood recedes, the available literature does not provide precise information on how long it normally takes for the foundation to regain its original strength. This is believed to depend on the type of material being deposited by live-bed streams. For example, cohesive materials such as clays may tend to regain their strength within a short period of time (perhaps 2 to 3 months). On the other hand, fine sands may take much longer to consolidate and regain their original strengths. As a compromise, for this illustrative example, we will assume that it will take about 6 months (½ year) for a foundation to regain its original strength. We will assume that the scour depth produced by the maximum yearly flood will remain at its maximum value for this half-year period. This assumption will also indirectly account for the effects of smaller floods within that period of time. In the proposed model, we will also assume that the scour depth will be reached instantaneously as the flood occurs and that the flooding period is always long enough for the maximum scour depth to be reached.

Using these assumptions, the proposed model for occurrence of scour can be represented as shown in Figure 3. *T* is

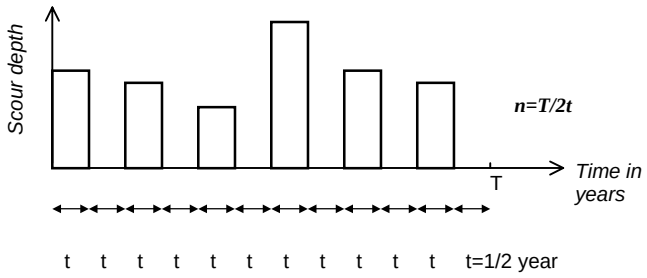

Figure 3. Representation of proposed scour model.

the lifetime of the bridge (e.g., 75 years), t is equal to the duration of the maximum scour (½ year) for each time unit (1 year). n is the number of scour occurrences within the time period T (or number of scour repetitions). For the 75-year design life of a bridge, $n = 75$, assuming one flooding season per year.

The model represented in Figure 3 can be used to calculate the reliability of a foundation subjected to scour alone or to the combination of scour and other extreme events. The reliability calculations for scour alone are illustrated in Section 2.1 in this appendix. The reliability calculations for the combination of scour and earthquake loads are illustrated in Section 5. In order to illustrate the load combination problem, a reliability model for earthquake alone is needed. Such a model is presented in Section 4.

2.1 Reliability Analysis for Scour Alone

The model used herein for the reliability analysis of a bridge foundation subjected to scour alone is based on the example provided in Appendix B of the interim report for NCHRP Project 12-48. The calculations use the following assumptions:

1. The probability distribution for the maximum 1-year flood is expressed as $F_Q(x)$, which gives the cumulative probability that the 1-year discharge volume, Q, is less than x. The cumulative probability distribution of the maximum 1-year discharge volume Q follows a log-normal distribution. This is based on probability plots and K-S goodness-of-fit tests.
2. A 75-year design life (return period) is assumed in order to be consistent with the AASHTO LRFD specifications.
3. The maximum 75-year flood discharge has a cumulative probability distribution $F_{Q75}(x)$ related to the probability distribution of the 1-year maximum discharge by

$$F_{Q75}(x) = F_Q(x)^{75}. \tag{8}$$

Equation 8 assumes independence between the floods observed in different years. This assumption is consistent with current methods to predict maximum floods.

4. For a specific discharge rate Q, the corresponding values for the flow velocity V and flow depth y_0 can be calculated by solving Equation 7 for y_0 and then using Equation 5 to find V.
5. It is noted that determining the appropriate Manning roughness coefficient (n in Equations 5 and 7) is associated with a high level of uncertainty. Therefore, in this example, we will assume that n is a random variable with a mean value equal to 0.025 (the recommended value for smooth earth surfaces) and a coefficient of variation equal to 28%. The 28% COV was adapted from the Hydraulic Engineering Center (1986), which recommends that n follow a lognormal distribution with a COV ranging from 20% to 35% (with an average value of 28%). It is herein assumed that the slope S is known and, thus, the uncertainties in V are primarily due to the uncertainties in determining n.
6. For any set of values for V and y_0, one can calculate the Froude number from Equation 2 and substitute these values into Equation 1 to find the 100-year design scour depth. Equation 1, however, as explained earlier, gives a safe value for the depth of scour. The average value was found by Johnson (1995) to be about 0.55 times the nominal value (bias value is 0.55). Also, the ratio of the true scour value over the predicted value has a COV of 52%. This bias is represented by a modeling parameter λ_{sc}. Thus, the true scour value is given by an equation of the form

$$y_{\max} = 2\lambda_{sc} y_0 K_1 K_1 K_1 K_1 \left(\frac{D}{y_0}\right)^{0.65} F_0^{0.43} \tag{9}$$

7. It should be noted that Johnson (1995) also recommends that the factor K_3, representing the effect of streambed condition, be treated as random variable with a bias equal to 1.0 and a COV equal to 5%.
8. Data on the type of the probability distributions for λ_{sc} and K_3 are not available. In the interim report for this project, Johnson proposed to use triangular distributions. It is herein assumed that n will follow a lognormal distribution as recommended by the Hydraulic Engineering Center (1986). This will ensure that n does not take values less than 0. On the other hand, because it is unlikely that λ_{sc} and K_3 will have upper or lower bounds, we shall herein assume that these two random variables follow normal (Gaussian) distributions. Note that triangular distributions where assumed in the interim report for both these variables. A sensitivity analysis will be performed at a later stage of this project to study how these assumptions will affect the final results.

The information provided above can be used in a simulation program to find the probability that the scour depth in a 75-year period will exceed a given value y_{cr}. A summary of the input data used in a Monte Carlo simulation program that calculates the probability that the actual scour depth will exceed a critical value is shown in Table 3.

The probability that y_{max} will exceed a critical scour depth, y_{cr}, is calculated for different values of y_{cr} as shown in Figure 4 for all five rivers. This data are also summarized in Table 4. The results of the simulation can be summarized as shown in Table 4 for the five rivers. It is observed that the safety index implied in current scour design procedures is on the order of 1.40 to 1.50, which is much lower than the 3.5 safety index used as the basis for the calibration of the load factors for the combination of live and dead loads.

Table 5 gives the load factor that should be applied on the scour design equation in order to produce different values of reliability indexes. For example, if a target reliability index of $\beta_{target} = 3.50$ is desired, then the average load factor that should be used in designing bridge foundations for scour should be equal to 1.69. Similarly, if a reliability index $\beta_{target} = 2.50$ is to be used as the target index for the design of bridge foundations for scour, then the load factor should be equal to 1.32. This means that a "load" (safety factor) equal to 1.69 to satisfy a target index of 3.5 or equal to 1.32 to satisfy a target index of 2.50 should further multiply the scour depth obtained from Equation 1. The load factors for other target safety index values ranging from 4.0 to 2.0 are provided in Table 5.

2.2 Final Remarks

The reliability calculations shown above assumed a deterministic value of y_{cr}. In general the critical depth, y_{cr}, that will produce the failure of the foundation is a random variable that depends on the foundation type, soil properties, and the type of loading (lateral or vertical) applied on the structure. For example, under the effect of lateral loads, pile foundations may fail in shear or in bending. Probability of failure would increase in the presence of scour that extends the moment arm of the lateral load. In addition, scour would decrease the depth of the remaining soil available to resist the applied moment and shear forces. On the other hand, when a dynamic analysis is performed, it is observed that the presence of scour reduces the stiffness of the bridge foundation

TABLE 3 Input data for reliability analysis for scour alone

Variable	Mean value	COV	Distribution Type
Q—maximum 75-yr discharge rate	As provided in Table 1	As provided in Table 1	Lognormal
λ_Q modeling variable for Q	1	5%	Normal
n Manning roughness	0.025	28%	Lognormal
λ_{SC} modeling variable	0.55	52%	Normal
K_3 Bed condition factor	1.1	5%	Normal

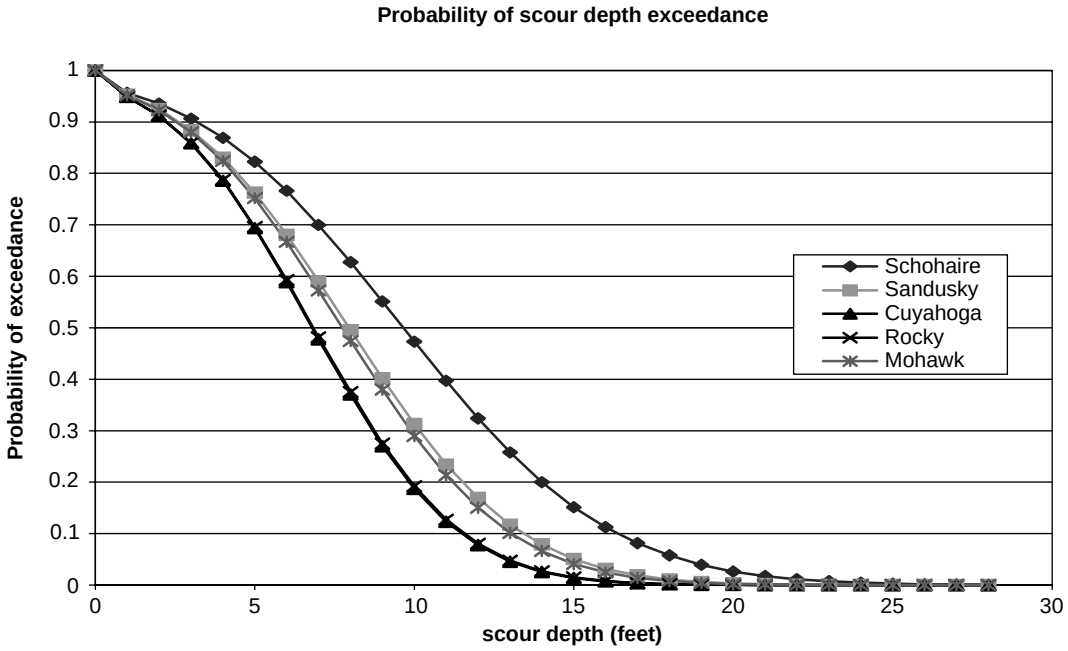

Figure 4. Probability that actual scour will exceed critical depths.

TABLE 4 Summary of simulation results

River	Average Q_{75yr} (Q for 75 years) (ft3/sec)	COV of Q_{75yr}	Average y_{s75} (max.scour depth in 75 yrs)	COV of Y_{s75}	Design depth (ft)	Reliability index β
Schohaire	85,000	29%	9.8	52%	17.3	1.40
Mohawk	34,000	12%	7.8	51%	14.0	1.51
Sandusky	38,000	18%	8.0	51%	14.3	1.41
Cuyahoga	20,000	16%	6.9	51%	12.3	1.42
Rocky	21,000	19%	6.9	51%	12.3	1.40

TABLE 5 Design scour depths required to satisfy target reliability levels

Target index	β = 4.0		β = 3.5		β = 3.0		β = 2.5		β = 2.0	
Required depth (ft)	Depth	Load factor	Depth	Load factor	Depth	Load factor	Depth	Load factor	Depth	Load factor
River										
Schohaire	33.5	1.90	30.0	1.73	26.0	1.50	23.0	1.33	20.0	1.15
Mohawk	26.0	1.86	23.0	1.64	20.5	1.46	18.5	1.32	16.0	1.14
Sandusky	26.5	1.85	24.0	1.68	21.0	1.47	19.0	1.33	17.0	1.19
Cuyahoga	22.0	1.79	20.5	1.67	18.0	1.46	16.0	1.30	14.0	1.14
Rocky	23.0	1.87	21.0	1.71	18.0	1.46	16.0	1.30	14.0	1.14
Average		***1.85***		***1.69***		***1.46***		***1.32***		***1.15***

thus creating a more flexible system that often leads to a reduction in dynamic loads. The example solved in the next section of this report will illustrate how the lateral load will affect the safety of bridges for different failure modes.

The controlling random variable for the reliability analysis is the modeling factor λ_{sc}, which has a high COV of 52%. This COV is higher than that of the maximum 75-year flood, which is about 15%. It should be noted that the analysis performed for scour alone produces a reliability index and probability of failure values that are totally independent of the time period during which the scour hole is at its maximum depth. The effect of the scour duration will be important as we study the reliability of bridge piers due to the combined effects of scour and other loads. Section 3 will analyze the bridge described in Figure 1 for earthquake loads using current analysis methods. Section 4 will develop a model for the reliability analysis of bridge piers subjected to earthquake loads alone. Section 5 will demonstrate the reliability analysis for the combination of earthquake loads and scour.

3. ANALYSIS OF BRIDGE FOR EARTHQUAKE LOADS

In this appendix, we are illustrating the case in which scour is to be combined with seismic forces. In order to study the combination problem, we first perform a deterministic analysis of the bridge under the effect of seismic forces to determine the nominal design forces and moments. In Section 4, the reliability of the column subjected to seismic forces alone is executed. In Section 5, the reliability analysis is expanded to demonstrate how the combination of scour and earthquakes will affect the reliability of the column and the foundation. The reliability analysis will be used to develop load factors that will be calibrated to achieve consistent target reliability levels. A first attempt on the calibration is presented in Section 6.

3.1 Bridge Geometric Properties

The bridge example studied in this section consists of three spans (60 ft, 100 ft, 60 ft) as illustrated in Figure 1 of Section 1.1. The bridge has two bents, each of which is formed by a 6-ft-diameter column. The weight applied on each bent is calculated to be 1,527 kips divided as follows: superstructure weight = 979 kips, weight of substructure = 322 kips, and weight of wearing surface = 2.46 kip/ft. Following current practice, the tributary length for each column is 91.9 ft where 50 ft is 50% of the distance between the columns and 41.9 ft is 70% of the distance between the column and the external support. This assumes that the lateral connection of the superstructure to the abutments will not break because of the earthquake lateral motions. The clear distance between the base of the column and the center of the superstructure is 25 ft. The foundation consists of a pile shaft (pile extension) that extends 50 ft into the soil. The soil is assumed to have an elastic modulus of Es = 10,000 psi corresponding to moderately stiff sand. The point of fixity of the floating foundation can be calculated using the relationship provided by Poulos and Davis (1980), given as follows:

$$\left(\frac{L_e}{L}\right)^3 + 1.5\frac{e}{L}\left(\frac{L_e}{L}\right)^2 = 3K_R\left(I_{\rho H} + \frac{e}{L}I_{\rho M}\right) \qquad (10)$$

where

L_e = the effective depth of the foundation (distance from ground level to point of fixity);
L = the actual depth;
e = the clear distance of the column above ground level;
K_R = the pile flexibility factor which gives the relative stiffness of the pile and soil;
$I_{\rho H}$ = the influence coefficient for lateral force; and
$I_{\rho M}$ = the influence coefficient for moment.

The pile flexibility factor is given as follows:

$$K_R = \frac{E_p I_p}{E_s L^4}. \tag{11}$$

If the pile is made of 4,000 psi concrete, then E_p equaling 3600 ksi (= $57[4000]^{1/2}$) and the diameter of the column being D = 6 ft results in a moment of inertia I_p = 63.62 ft^4 (= $\pi r^4/4$). Thus, for a pile length of 50 ft, the pile flexibility becomes

$$K_R = \frac{E_p I_p}{E_s L^4} = \frac{3{,}600{,}000 \times 63.64}{10{,}000 \times 50^4} = 0.037. \tag{11′}$$

The charts provided by Poulos and Davis (1980) show that for K_R = 0.0037, the influence coefficients $I_{\rho H}$ and $I_{\rho M}$ are respectively on the order of 5 and 15. This will produce an equation of the following form:

$$\left(\frac{L_e}{50}\right)^3 + 1.5\frac{25}{50}\left(\frac{L_e}{50}\right)^2 = 3 \times 0.0037 \times \left(5 + \frac{25}{50}50\right) \tag{10′}$$

where the value of e = 25 ft, which is the clear height of the column.

The root of this equation produces a ratio of L_e/L = 0.35, resulting in an effective depth of 18 ft below ground surface. Thus the effective total column height until the point of fixity becomes 25 ft + 18 ft = 43 ft.

For transverse seismic motion, the bent is assumed to be fixed at the base of the effective pile depth and free on the top. Thus, the bent stiffness is

$$K_{bent} = \frac{3EI}{H^3} \tag{12}$$

where

H = the effective column height ($H = e + L_e$),
E = the column's modulus of elasticity, and
I = the moment of inertia.

For typical concrete columns, E equals 3,600 ksi. For a circular column with a diameter of D = 6 ft, the moment of inertia is

$$I = \frac{\pi r^4}{4} = \frac{\pi 3^4}{4} = 63.64\, ft^4. \tag{13}$$

For a height equal to 45 ft, Equation 13 gives the bent stiffness as follows:

$$K_{bent} = \frac{3EI}{H^3} = \frac{3 \times 3600\text{k/in}^2 \times 144\text{ft}^2/\text{in}^2 \times 63.64\text{ft}^4}{(43\text{ft})^3} = 1244 \text{ kip/ft}. \tag{12′}$$

The natural period of the bent system, T is

$$T = \frac{2\pi}{\omega} = 2\pi\sqrt{\frac{M}{K}} = 2\pi\sqrt{\frac{1527 \text{ kip/32.2 ft/sec}^2}{1244 \text{ kip/ft}}} = 1.23 \text{ sec} \tag{14}$$

where

ω = the circular frequency of the system;
M = the mass ($M = W/g$ where W is the weight and g is the acceleration of gravity); and
K = the stiffness.

According the AASHTO LRFD specifications, the elastic seismic response coefficient C is given by

$$C = \frac{1.2AS}{T^{2/3}} \le 2.5A \tag{15}$$

where

A = the acceleration coefficient (the seismic acceleration as a multiple of the acceleration of gravity),
S = the soil type parameter, and
T = the natural period of the system.

The AASHTO LRFD specifications (Figure 3.10.2-2 of the manual) provide maps that give seismic acceleration for different regions of the United States. For example, for bridges to be located in the New York City area, the map of the acceleration coefficients shows a value of A on the order of 15% to 18% of g. Current trends in earthquake design of highway bridges are favoring the use of the National Earthquake Hazards Reduction Program (NEHRP) spectra, and a new earthquake design specification for bridges is proposing to use the same NEHRP spectra developed for buildings. For this reason, this appendix is based on using the NEHRP spectra rather than the current AASHTO specifications. The sections below illustrate the application of the NEHRP approach for the design of the bridge illustrated in Figure 1 of Section 1.1.

3.2 Earthquake Intensity

The USGS mapping project gives the peak ground accelerations (PGAs) at bedrock level and the corresponding spectral

values for 10%, 5%, and 2% probability of exceedance in 50 years for points throughout the United States. The spectral accelerations are given for periods of 0.2, 0.3, and 1.0 sec corresponding to the three different PGAs. Table 6 lists these values for the areas with the following zip codes: 10031 in New York City, 38101 in Memphis, 55418 in St. Paul, 98195 in Seattle, and 94117 in San Francisco. The spectral accelerations give the accelerations of the mass of a single-degree-of-freedom system that is supported by a system that has a natural period of 0.2, 0.3, or 1.0 sec when the acceleration at the base of the system is equal to the corresponding PGA. The values shown in Table 6 are in %*g* where *g* is the acceleration due to gravity. Table 6 shows the accelerations for three different probabilities of exceedance, namely 10% in 50 years, 5% in 50 years, and 2% in 50 years. For example, the 2% in 50 years corresponds to an earthquake return period of 2,500 years. The 10% in 50 years corresponds to a return period of 500 years. These return periods are normally used as the bases of current bridge design practice.

3.3 NEHRP Earthquake Response Spectrum

The spectral accelerations provided in Table 6 are for single-degree-of-freedom (SDOF) systems founded on bedrock. The values are given for only three natural periods—0.2, 0.3, and 1.0 sec—in addition to the PGA. NEHRP has proposed a method to use the information provided in Table 6 to develop acceleration response spectra that are valid for various soil conditions and for systems with different natural periods. The NEHRP response spectra can be described by a curve with the shape shown in Figure 5. In Figure 5, S_a is the spectral acceleration, T is the natural period of the system, S_{Ds} is the maximum spectral acceleration, and S_{Dl} is the spectral acceleration for a period of $T = 1$ sec. All spectral accelerations are given as function of g, the acceleration due to gravity. T_0 gives the period at which the maximum spectral acceleration is reached. T_s gives the period at which the spectral acceleration decreases below the maximum value. When the period T is less than T_0, the spectral acceleration increases linearly. When the period T is greater than T_s, the spectral acceleration is inversely proportional to T. The values of S_{Ds} and S_{Dl}, as well as T_0 and T_s, are calculated from the spectral accelerations given in Table 6 and the soil properties as described further below.

TABLE 6 Probabilistic ground motion values, in %*g*, for five sites (based on USGS website)

Site	10% PE in 50 yr	5% PE in 50 yr	2% PE in 50 yr
S.Francisco			
PGA	52.65	65	76.52
0.2 sec SA	121.61	140.14	181
0.3 sec SA	120.94	140.44	181.97
1.0 sec SA	57.7	71.83	100.14
Seattle			
PGA	33.77	48.61	76.49
0.2 sec SA	75.2	113.63	161.34
0.3 sec SA	62.25	103.36	145.47
1.0 sec SA	22.06	32.23	55.97
St. Paul			
PGA	0.76	1.31	2.5
0.2 sec SA	1.82	3.17	5.63
0.3 sec SA	1.61	2.72	4.98
1.0 sec SA	0.73	1.38	2.66
New York			
PGA	6.32	11.92	24.45
0.2 sec SA	12.59	22.98	42.55
0.3 sec SA	9.42	16.64	31.17
1.0 sec SA	2.85	5.11	9.4
Memphis			
PGA	13.92	30.17	69.03
0.2 sec SA	27.46	58.71	130.03
0.3 sec SA	20.38	43.36	110.62
1.0 sec SA	6.46	15.47	40.74

The first step in the earthquake analysis process is to develop the spectral response curve of Figure 5. This requires the identification of the foundation soil type. Having a modulus of elasticity on the order of 10,000 psi would classify the site condition as stiff soil (NEHRP Soil Category D). This information will be used to obtain the site coefficients (or site amplification factors).

For a 500-year return period (10%PE in 50 years), the mapped spectral acceleration, S_s, for the short period of $T = 0.2$ sec is taken from Table 6 for each of the five sites. Similarly, the spectral acceleration S_1 for a period of $T = 1$ sec is obtained from Table 6 for each site. The site coefficients are obtained from the NEHRP provisions as F_a for short periods and F_v for 1 sec from Table 4.1.2.4.a and 4.1.2.4.b of NEHRP (1997). Thus, the maximum earthquake spectral response accelerations for short period (0.2 sec) S_{MS} and for the 1-sec period S_{M1} adjusted for the proper soil profile are obtained from

$$S_{MS} = F_a S_S \qquad \text{and} \qquad S_{M1} = F_v S_1. \tag{16}$$

NEHRP allows for a $^2/_3$ (= 0.667) correction on the maximum earthquake accelerations. Thus, the critical amplitudes on the response spectrum are

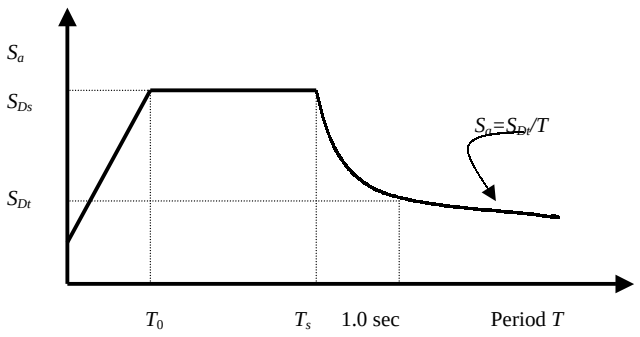

Figure 5. NEHRP design response spectrum.

$$S_{MS} = 0.667 S_{MS} = 0.667 FaS_S \quad \text{and}$$
$$S_{M1} = 0.667 S_{M1} = 0.667 F_V S_1. \tag{17}$$

All spectral values are given in function of the acceleration due to gravity, g. Critical periods on the response spectrum (see Figure 5) are

$$T_0 = 0.20 S_{D1}/S_{DS} \quad \text{and} \quad T_S = S_{D1}/S_{DS} \tag{18}$$

The equation describing the acceleration response spectrum, S_a, shown in Figure 5 will be

$$\begin{aligned} S_a &= 0.6\frac{S_{DS}}{T_0}T + 0.40 S_{DS} && \text{for } T < T_0 \\ S_a &= S_{DS} && \text{for } T_0 < T < T_s \\ S_a &= \frac{S_{D1}}{T} && \text{for } T > T_s \end{aligned} \tag{19}$$

For the 2,500-year return period (2%PE in 50 years), the mapped maximum earthquake spectral response for short periods, S_s, are also taken from Table 6, and the determination of the spectral curve is executed following Equations 16 through 19 for each of the five sites. The site coefficients, F_a and F_v (site amplification factors), are also obtained from the NEHRP provisions. The maximum earthquake spectral response accelerations adjusted for the proper soil profile are given in Table 7 for the five sites studied for a natural period of $T = 1.23$ sec, which is the period of the system studied in this example.

3.4 Design Moment Capacity of Column

Using a response modification factor of $R = 2.0$ for single columns of essential structures, the applied design forces and moments are reduced by $R = 2.0$ to account for column ductility. The equivalent force on the top of the column is obtained by multiplying the weight by the spectral acceleration (S_a) corresponding to the natural period of $T = 1.23$ sec. The moment at the base of the pile shaft is obtained by multiplying the equivalent force by the effective column height H. Thus, the final design moment in the column is obtained as follows:

$$M_{\text{design}} = \frac{WS_aH}{R}. \tag{20}$$

The weight applied on the bridge column W is 1,527 kips. The spectral acceleration values are taken from Table 7. The effective height of the column, H, includes the clear height plus the depth to the point of fixity ($H = e + L_e = 25$ ft + 18 ft = 43 ft). Using Equation 20, the design moments for the column are calculated as given in Table 8.

3.5 Check of Foundation Safety

The design of the foundation should be such that the soil must be able to resist either the elastic forces applied on the bridge system or the forces produced from the plastic hinging of the column. The smaller of the two resulting forces is used for designing the depth of the bridge foundation, implying that if the earthquake forces induce the formation of the plastic hinge in the column, then only the forces transmitted by the hinge need to be considered for the soil resistance. It is only in the case in which the columns are so overdesigned that no hinges will form in them that the soil needs to carry the full elastic forces applied on the bridge system.

For piles in cohesionless soils, the depth of the pile bent should be such that the soil pressure resists the applied lateral forces. Using the Broms model as described by Poulos and Davis (1980), the lateral load capacity of the soil is given by

$$H_u = \frac{0.5\gamma D L^3 K_p}{e + L} \tag{21}$$

where

γ = the soil's specific weight;
L = the depth of the foundation;
D = the diameter of the foundation;
e = the column eccentricity above ground level; and
K_p = Rankine's passive pressure coefficient, given by

$$K_p = \frac{1 + \sin\phi}{1 - \sin\phi} \tag{22}$$

where ϕ is the angle of internal friction of the soil.

TABLE 7 Spectral accelerations, S_a, for 10% and 2% PE in 50 years for bridge column (based on NEHRP specifications)

Site	10%PE in 50 yr	2%PE in 50 yr
San Francisco	0.469	0.814
Seattle	0.234	0.455
St. Paul	0.009	0.035
New York	0.037	0.122
Memphis	0.084	0.352

TABLE 8 Design moments for 10% and 2% PE in 50 years (based on NEHRP specifications)

	10% PE in 50 yr (kip-ft)	2% PE in 50 yr (kip-ft)
San Francisco	15397.5	26724.03
Seattle	7682.34	14937.88
St. Paul	295.47	1149.07
New York	1214.73	4005.32
Memphis	2757.76	11556.34

For design purposes, the applied lateral force resulting from the formation of the plastic hinge in the bridge column is obtained from the over strength moment capacity of the column, which is 1.3 times the plastic moment capacity (i.e., 1.3 times the values shown in Table 8).

If the clear column height is $e = 25$ ft and the effective depth to the point of fixity is $L_e = 18$ ft with $H = 43$ ft ($H = e + L_e$), then the equivalent shearing force produced in the hinge accounting for the column's over strength will be

$$H_{\text{applied}} = \frac{1.3M_p}{H} \tag{23}$$

where M_p is taken from Table 8. Using this information, the required foundation depth for each site is given as shown in Table 9.

Notice that the calculations of the effective depth and the applied moment performed above during the determination of the column design capacity assumed a foundation depth of 50 ft. The results of Table 9 show that the 50-ft depth is conservative for most bridge sites. It is also noted that the point of fixity for the bridge/foundation system under lateral loads is on the order of 16 to 18 ft for all foundations exceeding 30 ft in actual depth. An iterative process may be used to find the optimum foundation depth as a function of site information. In addition to resisting the lateral load, the foundation depth should be such that the pile be able to carry the applied vertical loads due to the dead weight of the structure and the live load expected during its design life. The required foundation depth to resist the vertical loads is calculated in Section 3.6. The reliability calculations performed in Section 4 studies the effect of different column depths on the safety of bridge columns against the failure of the column in bending and the bearing capacity of the foundation.

3.6 Safety Check of Foundation for Vertical Loads

In addition to carrying the horizontal load produced by the earthquake tremors, the foundation should be able to carry the vertical loads applied on the structures including the dead weight of the superstructure and substructure as well as the vertical live load. Piles resist the vertical loads caused by the combination of friction resistance and bearing resistance.

TABLE 9 Required foundation depth based on column capacity

Site	Required foundation depth (ft)	
	10% PE in 50 yr	2% PE in 50 yr
San Francisco	34.7	43.7
Seattle	26.2	34.3
St. Paul	7.6	12.5
New York	12.8	20.2
Memphis	17.5	30.8

The friction and bearing resistances are a function of the pile dimensions and soil properties. In the case studied herein, the angle of friction for sandy soil is taken as $\phi = 35°$, the modulus of elasticity as $E_s = 10{,}000$ psi, the Poisson ratio as $\nu = 0.3$, the unit weight as $\gamma = 60$ lb/ft^3, and the pile diameter as $D = 6$ ft. Poulos and Davis (1980) show that the vertical stress in the soil will vary linearly up to a level of $z = 7$ times the pile diameter, $z = 7D$. This means that the stress will vary linearly up to 42 ft below ground level, after which point the stress remains constant. For saturated soils, the maximum pressure will be due to the combination of water and soil weights, thus the maximum stress will be $\sigma_v = 42$ ft $\times$ 60 lb/ft^3 = 2,520 lb/ft^2. For bored piles with $\phi = 35°$, the bearing capacity factor N_q is given by Poulos and Davis (1980) as $N_q = 40$. Thus, the bearing capacity of the pile, P_{bu}, at the 42-ft level and below will be as follows:

$$P_{bu} = A_b \sigma_v N_q \tag{24}$$

where A_b is the pile base diameter. For $A_b = 28.27$ ft^2 ($= \pi D^2/4$), $\sigma_v = 2{,}520$ lb/ft^2, and $N_q = 40$, the bearing capacity of the pile at the 42-ft depth and below is $P_{bu} = 2.85 \times 10^6$lb or 2,850 kips. The friction force, P_{su}, for up to z ft in depth is given by

$$P_{su} = \frac{\pi D(\sigma_v K_s \tan\phi)z}{2}. \tag{25}$$

The value of $K_s \tan\phi = 0.20$ is provided by Poulos and Davis for a friction angle $\phi = 35°$ and for bored piles. Thus, the friction force P_{su} for a depth of $z = 42$ ft will be equal to 200 kips. After the 42-ft depth, the friction force will be a constant function of $L - 42$ ft. This means that the total friction force will be 200 kips + 9.50 ($L - 42$).

The combination of P_{su} and P_{bu} should be able to carry the applied vertical loads from the superstructure as well as the weight of the pile. Thus, the final bearing capacity P_u is given as

$$P_u = 2{,}850 \text{ kips} + 200 \text{ kips} + 9.50 \text{ kip/ft } (L - 42 \text{ ft}). \tag{26}$$

Given a pile of length, L, the weight of the pile will be 150 lb/ft$^3 \times L \times \pi D^2/4$. The applied weight of the structure had been earlier given as $W = 1{,}527$ kips.

According to the AASHTO LRFD specifications (1994), the live load applied on a continuous bridge is due to 90% of the AASHTO lane load plus 90% of the effects of two AASHTO design trucks. The reaction at the interior support due to these loads are on the order of 350 kips. Using the LRFD equation with a dead load factor $\gamma_d = 1.25$ and a live load factor $\gamma_l = 1.75$ results in a required bearing capacity resistance of

$$\phi P_{\text{req.}} = \gamma_d\, 1{,}527 + \gamma_l\, 350 = 2{,}520 \text{ kips}. \tag{27}$$

For the bearing capacity of piles in sandy soils, the AASHTO LRFD does not provide a resistance factor ϕ, although values on the order of $\phi = 0.50$ to 0.65 are recommended for clay soils depending on the models used for calculating the bearing capacity. A factor of $\phi = 0.80$ is used when the pile bearing capacity is verified from load tests. By comparing Equations 26 and 27, it is clear that the AASHTO LRFD criteria can be met for a pile length $L = 50$ ft only if pile tests are conducted to verify the bearing capacity of the pile shaft or when a bell at the bottom of the caisson is provided to extend the area. For this example, we are assuming that the 50-ft pile length is acceptable to carry the vertical loads. A sensitivity analysis is performed in the next section to study the effect of different pile lengths on the reliability of the bridge when subjected to earthquake loads.

4. RELIABILITY ANALYSIS OF BRIDGE FOR EARTHQUAKES

The purpose of the analysis performed in this section is to calculate the probability that the bridge designed in Section 3 for the different moment capacities will fail under the effect of earthquake forces within its intended 75-year design life. A 75-year return period is chosen in order to remain compatible with the AASHTO LRFD specifications. The corresponding reliability index, β, will also be calculated. The objective is to study the reliability of bridges designed following current practice and the NEHRP specifications under the effect of earthquake loads. In this section, the analysis is performed assuming no scour. The model is subsequently used in Section 5 to study the reliability of bridges under the combined effects of scour and earthquake loads.

In this section, we will assume that the bridge was designed as described in the previous section to withstand the earthquake loads observed at the five different sites identified above. In order to perform the reliability analysis, we will need to account for the uncertainties associated with each of the random variables that control the safety of the bridge. Assuming no scour, the random variables are identified as

1. Strength capacity of bridge column,
2. Intensity of the earthquake acceleration at the site,
3. Natural period of the column,
4. Mass applied on the column,
5. Seismic response coefficient, and
6. Response modification factor.

In addition, although not treated as a random variable, the frequency of earthquakes at the bridge site plays an important role in determining the reliability of the bridge for earthquake risk. Other factors such as the height and diameter of the column and other geometric and material parameters are associated with very small uncertainties and may be treated as deterministic values.

4.1 Column Strength Capacity

A single-column bridge pier subjected to earthquake loads can fail in a variety of modes. These include (1) failure due to the applied bending moment exceeding the moment capacity of the column (this mode should consider the interaction between bending and axial loads); (2) failure in shear; and (3) failure of the foundations. In this example, the reliability analysis procedure is illustrated for the failure of the column due to the applied bending moment.

The bridge columns under combined axial load and bending moment are normally designed such that the design point at the interaction curve remains below the balance point. In this example, we are ignoring the effects of vertical accelerations as is common in practical cases for short- to medium-length bridges. Hence, the uncertainty in evaluating the vertical load is small compared with that associated with determining the lateral forces (and bending moments). For this reason, we shall assume that the effects of the axial load on the uncertainties in determining the moment capacity are negligible.

According to Nowak (1999), the moment capacity of concrete members in bending is on the average higher than the nominal capacity by a factor of 14% (bias 1.14), and the standard deviation is 13%. The probability distribution of the moment capacity is taken to be lognormal (Nowak, 1999). The final values used in this example are those recommended by Nowak.

4.2 Frequency of Earthquakes

We shall assume that the bridge under consideration may be located in any of the five cities listed in Table 6. The USGS Seismic Hazard Mapping Project stipulates an earthquake occurrence rate for each of the areas. These values are then used by USGS to determine the maximum annual probability curve for earthquake intensities that are discussed in the next section.

4.3 Intensity of Earthquake Accelerations

Frequencies at which earthquakes exceed certain levels of PGAs are provided by the USGS in two different formats: (1) plots showing the probability of exceedance of maximum yearly earthquakes versus PGAs for a number of representative U.S. sites, and (2) tables giving the probability of exceeding given acceleration levels in 50 years. The plots are shown in Figure 6.

The frequency of exceedance in 50 years is related to the maximum yearly earthquake levels, as shown below. For example, if the frequency of exceeding an earthquake level of $0.53g$ is given as 10% in 50 years, this indicates that the probability that the maximum earthquake level in 50 years will be below $0.53g$ is $1.00 - 0.10 = 0.90$. This can be represented as follows:

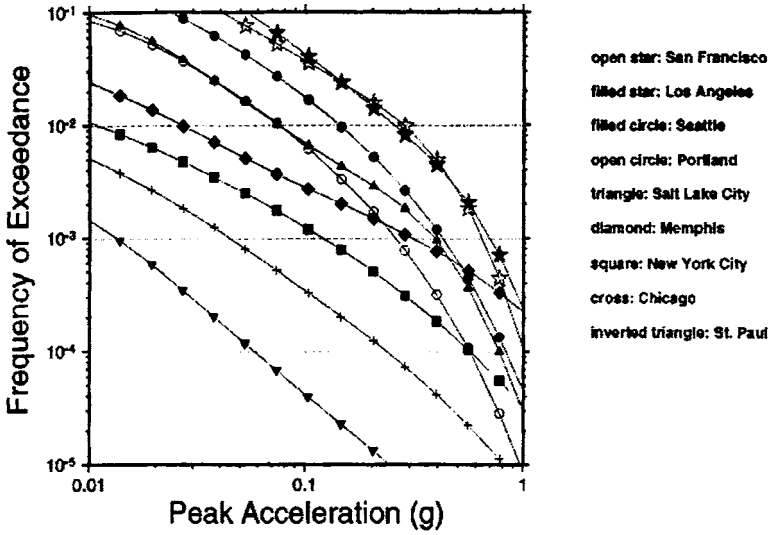

Figure 6. Annual probability of exceedance curves.

$$F_{A50}(0.53g) = 1.00 - 0.10 = 0.90 \quad (28)$$

where $A50$ is the maximum 50-year acceleration intensity and $F_{A50}(-)$ is the cumulative probability distribution of the maximum 50-year earthquake intensity. But, assuming independence between earthquake intensities (which is a common assumption in earthquake engineering practice), the 50-year probability of exceedance is related to the yearly probability of exceedance, $F_A(x)$, by

$$F_{A50}(x) = F_A(x)^{50}, \quad (29)$$

hence,

$$F_{A50}(0.53g) = (F_{A50}[0.53\text{g}])^{1/50} = 0.997895 \quad (30)$$

or the yearly probability of exceeding an acceleration of $0.53g$ is 0.2105% (1 – 0.997895 = 0.002105). Figure 6 gives the yearly probability of exceedance for a range of accelerations and a number of representative sites. These curves were developed by USGS and available at the USGS website for use in earthquake engineering practice.

In addition to the curves shown in Figure 6, the USGS Earthquake Hazard Mapping Project has provided the project with the data for the New York City, San Francisco, St. Paul, and Seattle sites. These data are entered in the reliability program to represent the earthquake intensity variable. The curve is fitted through a spline function to obtain a cumulative probability distribution that connects the data points. Since bridges are constructed for a 75-year design life, the probability of exceeding different acceleration levels in 75 years will be used in the reliability calculations. These values are obtained using an equation similar to Equation 29 but using an exponent equal to 75 in the right-hand side of the equation. Table 10 gives the values available for the five sites considered.

4.4 Natural Period of the Bridge

The natural period of a bridge depends on many parameters, including the type and the characteristics of the bridge foundation and the stiffness of the soil. Takada et al. (1989) have suggested that the average value of the period is about 1.08 times the value calculated using design methods (bias = 1.08) with a COV on the order of 20%. These values account for the soil structure interaction (SSI) and other analysis effects. The values provided by Takada et al. (1989) are primarily for buildings. The Takada et al. data should be applied on struc-

TABLE 10 Maximum yearly earthquake intensity levels versus probability of exceedance

	Frequency of Exceedance per Year			
Ground Motion (*g*)	New York	San Francisco	Seattle	St. Paul
0.005	1.74E-02	4.10E-01	2.27E-01	3.27E-03
0.007	1.37E-02	3.67E-01	2.04E-01	2.26E-03
0.0098	1.07E-02	3.17E-01	1.77E-01	1.50E-03
0.0137	8.29E-03	2.63E-01	1.48E-01	9.59E-04
0.0192	6.31E-03	2.06E-01	1.17E-01	5.86E-04
0.0269	4.72E-03	1.53E-01	8.69E-02	3.48E-04
0.0376	3.47E-03	1.09E-01	6.16E-02	2.03E-04
0.0527	2.49E-03	7.55E-02	4.14E-02	1.17E-04
0.0738	1.74E-03	5.11E-02	2.66E-02	6.80E-05
0.103	1.20E-03	3.41E-02	1.63E-02	3.97E-05
0.145	7.88E-04	2.25E-02	9.35E-03	2.29E-05
0.203	5.06E-04	1.50E-02	5.12E-03	1.33E-05
0.284	3.13E-04	9.63E-03	2.64E-03	7.55E-06
0.397	1.86E-04	5.52E-03	1.26E-03	4.17E-06
0.556	1.05E-04	2.44E-03	5.58E-04	2.19E-06
0.778	5.57E-05	7.30E-04	2.39E-04	1.08E-06
1.09	2.78E-05	1.36E-04	9.95E-05	4.95E-07
1.52	1.31E-05	1.67E-05	3.68E-05	2.10E-07
2.13	5.69E-06	1.48E-06	9.85E-06	8.02E-08

tural models that did not include the effects of SSIs as the 1.08 bias accounts for the effects of SSI. Since our analysis model included the effects of SSI, a lower bias should be used.

When SSI models are included in the analysis (as is the case in the models used in this section), the variation between the measured periods and the predicted periods appears to be smaller, and the bias is reduced to a value close to 1.0. This phenomenon is illustrated as shown in Figure 7 adapted from the paper by Stewart et al. (1999). The figure shows that, on the average, the predicted periods accounting for SSI are reasonably similar to the values measured in the field. The bias is found to be 0.99 and the COV on the order of 8.5%. It is noted that the SSI model shown in the figure is different than the model used in this section, and that the comparison is made for buildings rather than bridges. Also, it is noted that the study by Stewart et al. concentrated on the effects of SSI while the natural periods of the structural systems were inferred from field measurements. Thus, the uncertainties in modeling the structures were not included. Furthermore, many of the sites studied by Stewart et al. had relatively stiff soils where the effects of SSI are rather small.

Hwang et al. (1988) report that Haviland (1976) found that the median of natural periods for buildings is equal to 0.91 times the computed values with a COV of 34%. Chopra and Goel (2000) developed formulas for determining the natural periods of buildings based on measured data. The spread in the data shows a COV on the order of 20% for concrete buildings and slightly higher (on the order of 23%) for steel-frame buildings.

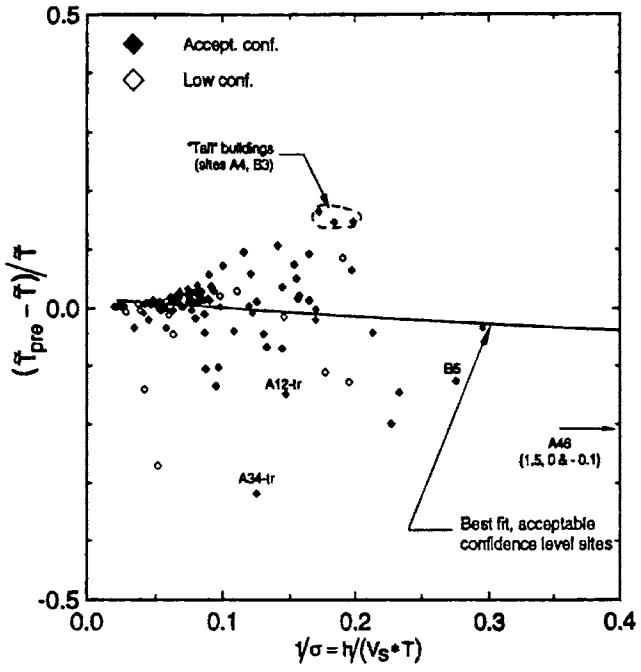

Figure 7. Variation of predicted natural period of the predicted foundation-soil system compared with measured values (from Stewart et al., 1999).

In this appendix, a sensitivity analysis is performed to study the effect of the variability of the natural *T* on the final results. The analysis shows that the final results are not sensitive to the values used for bias and COV on *T*. Based on the review of the above references, it is herein decided to use a bias of 0.90 and a COV of 20% for the period of the system. The 0.90 bias similar to that observed by Haviland (1976) is justified based on the fact that the analysis performed to calculate the period of the bridge system used the nominal value for the modulus of elasticity of the concrete, E_c. In reality, the actual modulus of the concrete will be higher than the nominal value and, thus, the predicted stiffness will be larger than the actual stiffness, producing a lower actual period than predicted. A correction factor of 1.20 to 1.30 on the concrete modulus is often used in engineering practice that would justify the 0.90 bias $\left(0.90 \approx 1/\sqrt{1.25}\right)$. The COV of 20% used herein corresponds to the values observed by Chopra and Goel (2000) for buildings. It may be argued that the prediction of the period for bridges may be less uncertain than that for buildings. However, the data collected by Chopra and Goel (2000) did not indicate any appreciable difference in the level of uncertainty due to building heights or sizes. Thus, it may be reasonable to assume that the COV on the period for bridges is also on the order of 20%. The proposed bias and COV are meant to account for both the uncertainties in the structural properties as well as the SSI.

4.5 Mass Applied on the Column

The dead weight effect on bridge members was found by Nowak (1999) to be on the order of 1.05 times the nominal (design) weight with a COV of 10%. This high COV, however, reflects the effects of the structural analysis as well as the uncertainty in estimating the weight. To account for the uncertainty in the weight alone, a COV of 5% is used. The probability distribution is assumed to be normal following the models used by Ellingwood et al. (1980) and Nowak (1999). It is noted that the variability in the mass and the weight considered here are used for calculating the applied forces and not the period. The uncertainty in predicting the mass during the calculation of the period is considered under the biases and COV of *T*.

4.6 Seismic Response Coefficient

The design spectra proposed for the upcoming AASHTO LRFD for earthquake design of bridge are similar to those adopted by NEHRP. These are based on the average response spectra developed by Frankel et al. (1997) from a large earthquake mapping project. Frankel et al. (1997) found that the level of confidence in NEHRP spectra is related to the number of earthquakes recently observed as well as to knowledge of the type and locations of the faults in a particular region.

For sites where a large number of earthquakes was observed, the COV is low; the COV is high for sites with few observed tremors. Frankel et al. provided maps showing uncertainty estimates for selected cities derived from Monte Carlo simulations. The data provided in this map show that the ratio between the 85th fractile and the 15th fractile for New York City is on the order of 5. Assuming a normal distribution, this means that the COV would be on the order of 30%. For the Memphis area, the ratio of the two fractiles is about 3, resulting in a COV of about 25%. For San Francisco, the projected COV is about 15%, and for St. Paul and Seattle the projections are that the COVs would be about 40% and 25%, respectively. Frankel et al. also show that the mean value of the spectral accelerations is very close to the uniform hazard spectra they developed and that resulted in the NEHRP specifications. It is noted that these observations are within the range of the values reported by Seed et al. (1976), who observed that the results of dynamic analyses using a variety of earthquake records resulted in a range of spectral responses with a COV of about 30% from the average spectra.

4.7 Response Modification Factor

The response modification factor is related to the ductility of the system. The purpose of the response modification factor is to allow for a linear elastic analysis of structural systems although the system may exhibit large levels of plastic deformations.

The response modification factor, *R*, is related to the ductility capacity of the bridge members. Thus, if a member's ductility capacity μ is known, the response modification for that member—assuming an SDOF system—may be evaluated so that the actual plastic response of the structure can be inferred from the linear elastic analysis. Miranda (1997) found that for typical periods of bridge systems (0.5 to 1.5 sec) subjected to a representative sample of earthquake records, the response modification, *R*, is on the average equal to the bridge column ductility capacity ($R = \mu$) with a COV of about 25%. This observation confirms the model first proposed by Newmark and Hall (1973) that was based on limited data from the El Centro Earthquake. The results of Miranda (1997) were calculated for a variety of sites with a range of soil classifications. Liu et al. (1998), in a report to the National Center for Earthquake Engineering Research (NCEER) and FHWA, found that the COV reduces to about 17% if the earthquake records were chosen to match those that produce the design spectral accelerations.

In addition to the issue of the relation between *R* and μ, another issue concerns the level of uncertainty associated with estimating the ductility capacity. Results given by Priestly and Park (1987) show that the real ductility of bridge columns are on the average about 1.5 times higher than the ductility estimated from the design formulas with a COV of about 30%. Thus, the actual response modification factor will be on the average 1.5 times the specified ductility capacity, $\mu_{\text{specified}}$, (a bias of 1.5), with a COV of 34% $\left(34\% = \sqrt{0.30^2 + 0.17^2}\right)$. The probability distribution for *R* is assumed to be normal.

The last issue with the response modification factor concerns the range of values specified for use during the design process by AASHTO and other earthquake design codes. For example, it is noted that the response modification factor specified by AASHTO for use during the analysis of single-column bents is set at 2.0, and 3.5 is used for multicolumn bents of essential structures while values of 3.0 and 5.0 are used for "other structures."ATC-6 mentions that an $R = 2.0$ is recommended for a wall-type pier "based on the assumption that a wall pier has low ductility capacity and no redundancy" (Applied Technology Council, 1981). It is clear that the difference among the 2.0, 3.0, 3.5, and 5.0 values of *R* used for the design of columns is not intended to account for the differences in the ductility capacities of the columns. Rather, the use of different values of *R* is meant to provide certain types of structures (particularly nonredundant and essential bridges) with higher levels of safety. In fact, since in all cases the design and construction procedures of columns in single-column bents or multicolumn bents are fairly similar, one would expect to find the ductility capacities of all columns to be about the same. It is noted that previous recommendations for the design of bridges under earthquake loads recommended that a response modification factor of $R = 8$ be used. In addition, tests on bridge columns performed at the University of Canterbury (Zahn et al., 1986) have shown that the ductility of properly confined columns can easily exceed 7.5 although some damage would be expected to occur.

On the other hand, the analysis of multicolumn bents produces different moments in each column due to the effect of the dead load and the presence of axial forces. An extensive analysis of different bent configurations founded on different soil types was performed for NCHRP Project 12-47 (Liu et al., 2001). The results showed that, due to the load redistribution and the presence of ductility, multicolumn bents on the average fail at loads up to 30% higher than the loads that make the first column reach its ultimate member capacity.

Based on the information collected from the references mentioned above, we will assume that the nominal ductility level of bridge columns will be equal to $\mu = R = 5.0$. The bias for the ductility level is 1.5 with a COV of 34%. This would results in a mean ductility value of $\mu = R = 7.5$. In addition, multicolumn bents will be associated with a "system overstrength factor" of 1.30 based on the work of Liu et al. (2001). It is noted that the values used herein are similar to those used by Hwang et al. (1988), who have recommended the use of a median value of $R = 7.0$ for shear walls with a COV of 40%.

4.8 Modeling Factor

The structural analysis produces a level of uncertainty in the final estimate of the equivalent applied moment on the base of

the bridge column. These factors include the effects of lateral restraints from the slab, the uncertainty in predicting the tributary area for the calculation of mass, the point of application of the equivalent static load, the variability in soil properties and the uncertainty in soil classification, the effect of using a SDOF model, the level of confidence associated with predicting the earthquake intensity, and so forth. Ellingwood et al. (1980) have assumed that the modeling factor has a mean value equal to 1.0 and a COV on the order of 20% for buildings. The same value is used in these calculations.

4.9 Reliability Equation

Using the information provided above, the applied moment on the bridge column is calculated using the following expression:

$$M_{\text{apl}} = \lambda_{\text{eq}} C' S_a(t'T) * \frac{A * W}{R} * H \tag{30a}$$

where

M_{apl} = the applied moment at the base of the column;
λ_{eq} = the modeling factor for the analysis of earthquake loads on bridges;
C' = the response spectrum modeling parameter;
A = the maximum 75-year PGA at the site (a 75-year design life is used to be consistent with the AASHTO LRFD specifications);
S_a = the calculated spectral acceleration as a function of the actual period;
T = the bridge column period;
t' = the period modeling factor;
W = the weight of the system;
R = the response modification factor; and
H = the column height.

The data used in the reliability analysis for the random variables of Equation 18 are summarized in Table 11. The variables not listed in Table 11 are assumed to be deterministic.

The final safety margin equation for earthquake loads applied on highway bridges can be represented as follows:

$$Z = M_{\text{cap}} - M_{\text{apl}} \tag{31}$$

where failure occurs if the safety margin Z is less than 0. M_{cap} is the moment strength capacity of the bridge column. Both M_{cap} and M_{apl} are random variables.

4.10 Reliability Results

Using a Monte Carlo simulation along with the safety margin of Equation 31 and the statistical data of Table 11, the reliability index for a 75-year design life of the bridge studied in this report is calculated for different foundation depths. The results illustrated in Figure 8 show that the reliability index is relatively insensitive to the depth of the pile foundation. This is because for the bridge soil type and pile diameter, the point of fixity remains relatively constant at about 16 ft to 18 ft below ground level when the foundation depth exceeds 35 ft. Thus, the stiffness of the system and the moment arm of the column are not affected by the depth of the foundation. Figure 8 also shows that the different sites produced nearly similar values of the reliability index (around 2.50) when the bridge has been designed for the 2% probability of exceedance in 50 years. This confirms that reasonably uniform hazards are achieved for bridge structures designed to satisfy the NEHRP specifications for various sites within the United States.

Figure 9 shows the reliability indexes obtained if the bridge were designed to resist the earthquake with a 10% probability of exceedance in 50 years. By comparing Figures 8 and 9, it is observed that the reliability index decreases to an average of $\beta = 1.90$ from an average of 2.50. Also, it is noted that the range of variation in the reliability index is wider for the lower earthquake level, the range being from about $\beta = 1.6$ to $\beta = 2.1$.

To study the effect of the uncertainties associated with calculating the natural period of the system on the reliability index, the reliability calculations are executed for three different cases with different biases and COVs on T. The

TABLE 11 Summary of input values for seismic reliability analysis

Variable	Mean	Bias	COV	Distribution Type
M_{cap}	From Table 8	1.14	13%	Lognormal
λ_{eq}	1.0	1.0	20%	Normal
C'	1.0	1.0	Varies per site (15% to 40%)	Normal
A	From Table 10	From Table 10	From Table 10	From Table 10
T	1.23 sec	0.9	20%	Normal
W	1527 kips	1.05	5%	Normal
R	5	1.5	34%	Normal

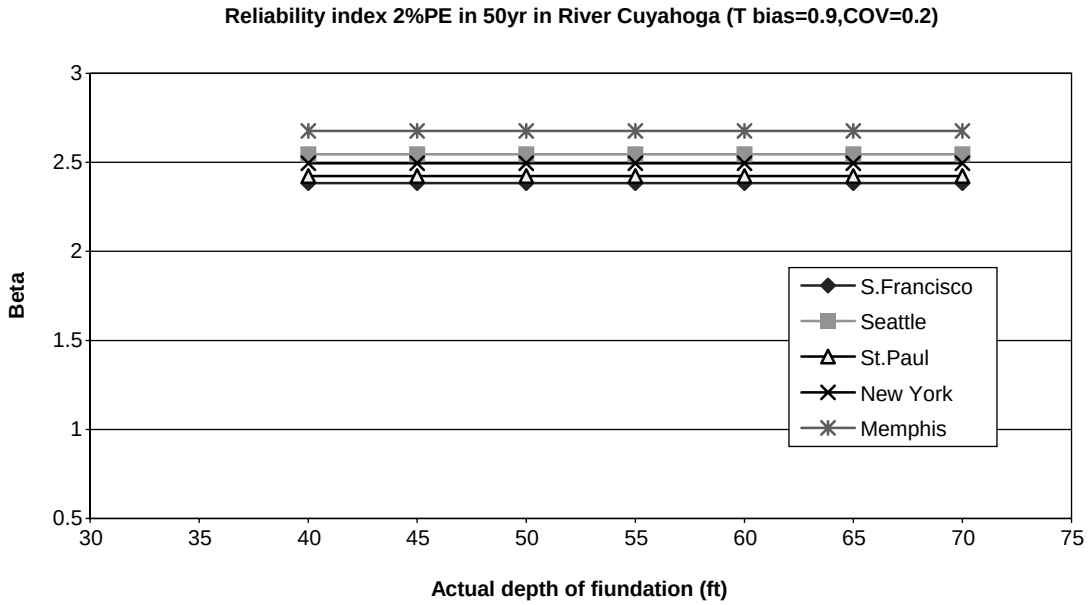

Figure 8. Reliability index versus foundation depth for bridges designed for the earthquakes with 2% probability of exceedance in 50 years.

results executed for the San Francisco site are illustrated in Figure 10. The results show that the final results are relatively insensitive to the variations in the input parameters for *T*. In fact, the calculations show that the uncertainties in determining the maximum earthquake intensity in a 75-year design life are dominant with a COV of 74% for the San Francisco site and even higher for the other sites (e.g., for New York City, the COV is about 280%). A previously performed first order reliability method (FORM) analysis has shown that the other important factor that affects the reliability index is the response modification factor, *R*, that is associated with a COV of 34%.

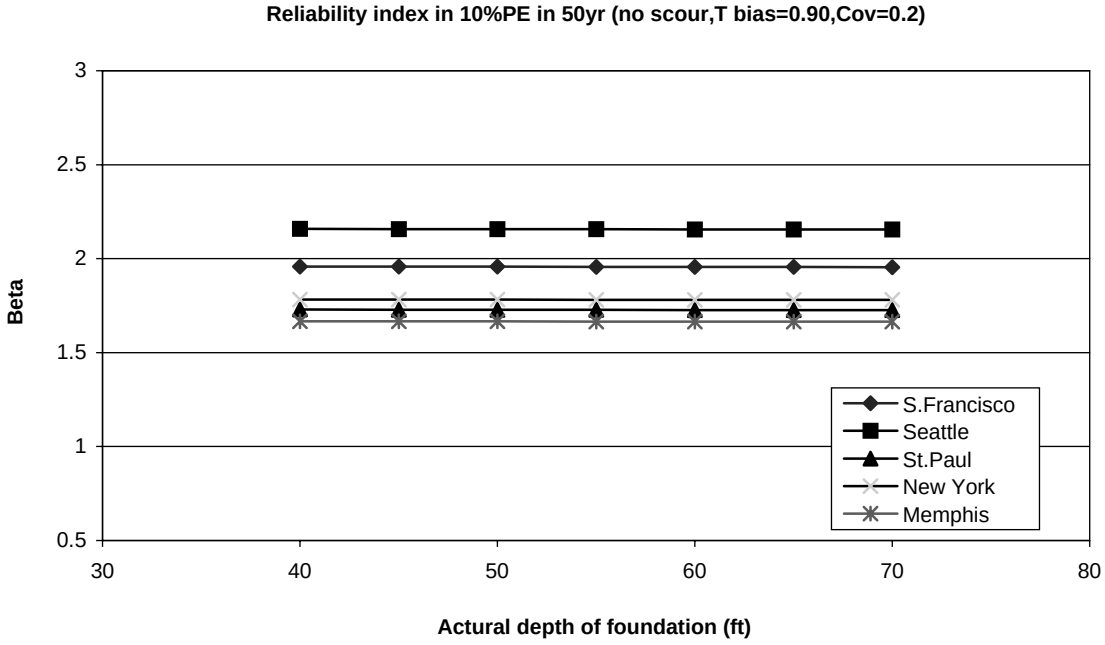

Figure 9. Reliability index versus foundation depth for bridges designed for the earthquakes with 10% probability of exceedance in 50 years.

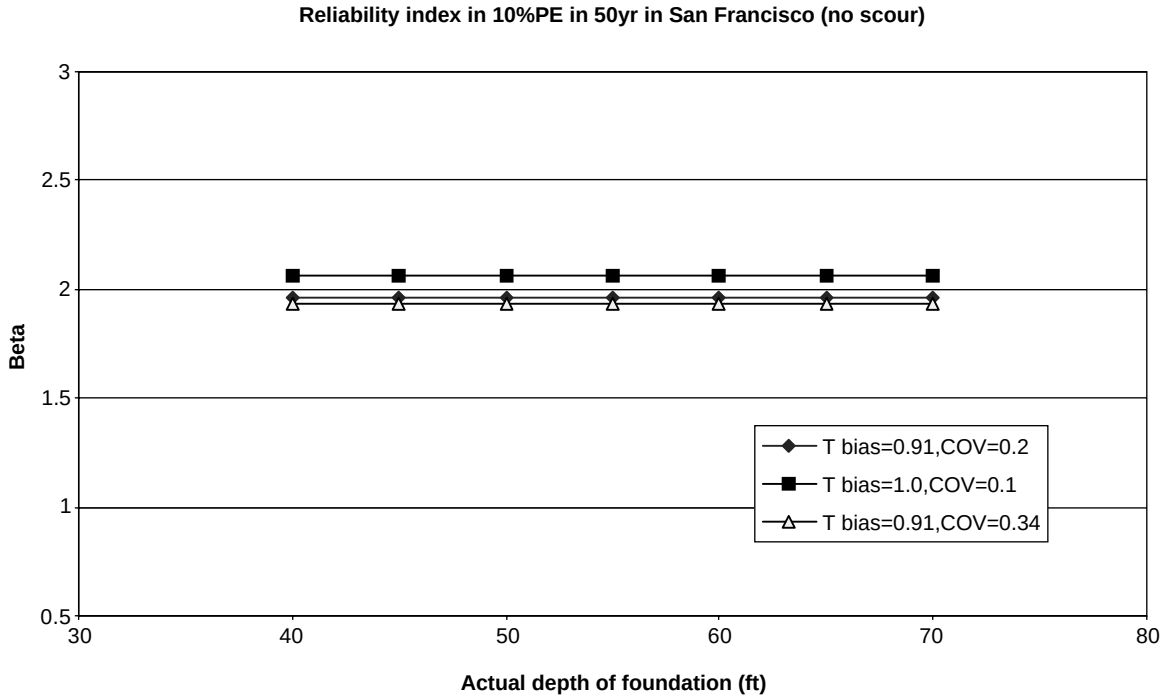

Figure 10. Sensitivity analysis for different biases and COV on the natural period T *(San Francisco).*

5. COMBINATION OF SCOUR AND EARTHQUAKES

5.1 Monte Carlo Procedure

The analysis of the safety of a bridge subjected to the combination of scour and earthquake loads is a function of the random variables identified in Sections 2 and 4 of this appendix and listed in Tables 3 and 11. Some of these variables vary with time, and others are constant over the design life of the bridge. The reliability analysis involving time-dependent variables in combination with time-independent random variables may be performed based on the Ferry-Borges model for load combination. The logic followed in formulating the combination problem is demonstrated in the following steps.

1. A bridge having the configuration shown in Figure 1 is designed to cross over the 220-ft-wide stream. The stream's characteristics provide a set of variables that are needed for the scour analysis. These characteristics are represented by the following random variables of Equation 9: Manning roughness coefficient, n; the streambed condition factor, K_3; and the modeling factors λ_{sc} and λ_Q. These variables are subject to scatter in their estimation, hence they are considered random. However, these variables remain the same throughout the design life of the bridge. On the other hand, the discharge rate Q is a random variable whose value changes from one flood to the other. Q is a time-dependent random variable.
2. Similarly, the geometric and other terms affecting the earthquake response of the bridge such as the weight, W, the variation in the estimated period, t', the response modification factor R, the modeling parameters λ_{eq} and the spectral modeling factor C', which are subject to scatter in their estimation and are herein treated as random variables. However, these variables remain the same throughout the design life of the bridge. On the other hand, the earthquake intensity A changes for each earthquake and, thus, like Q, A is also a time-dependent random variable.
3. The Monte Carlo simulation used to calculate the probability of bridge failure in a 75-year design life under the effect of the combination of scour and earthquake loads begins by randomly selecting values for each of the time-independent random variables listed above including the moment capacity (M_{cap}) that is treated as a time-independent random variable with a bias of 1.14 and a COV of 13%.
4. For every flooding season (assumed to be once a year), floods of random discharge intensities will occur in the stream crossed by the bridge described in Figure 1. The maximum annual discharge rate, Q, follows a log-normal distribution with different parameters depending on the river crossed by the bridge as described in Table 1.

5. Given a realization of the random variable Q, the corresponding flow depth, y_0, and velocity, V, are calculated from Equations 7 and 5.
6. For realizations of the modeling factors, λ_{sc} and λ_Q, the roughness factor, n, the bed condition factor, K_3, and the other deterministic parameters, the maximum expected scour depth for the 1 year, y_{max}, is calculated using Equation 9.
7. Since Q is a time-dependent random variable, then y_0 and V are also time-dependent random variables. Consequently, the maximum annual scour depth y_{max} is a time-dependent random variable.
8. The scour depth y_{max} is assumed to remain constant for the duration of the flooding season assumed to be $^1/_2$ year. During the next flooding season, the value of the scour depth may change depending on the occurrence of the random variable Q.
9. During the $^1/_2$ year period when y_{max} exists, there is a finite probability that an earthquake will also occur.
10. The probability distribution for the maximum earthquake intensity for this $^1/_2$-year period can be obtained from the results of Table 10 by using the relationship

$$F_A(x) = F_{A1yr}(x)^{1/2} \tag{32}$$

where A is the maximum earthquake intensity expected in the $^1/_2$-year period when scour is present, and A_{1yr} is the maximum earthquake intensity in 1 year as given in Table 10 for each site considered.

11. Given a realization of the scour depth, y_{max} obtained from the scour calculations based on the maximum discharge rate corresponding to 1 year, the effective height of the bridge column becomes

$$H = 25 \text{ ft} + y_{max} + L_e \tag{33}$$

where 25 ft is the original column height, y_{max} is the scour depth, and L_e is the distance between the ground level and the point of column fixity. The point of fixity is calculated from Equation 10 when the actual depth of the foundation, L, is adjusted by reducing the original depth by y_{max}.

12. The change in column height will produce a change in the stiffness K of Equation 12 and, consequently, will produce a change in the period of the system. (This change would reduce the natural period of the system and thus reduce the earthquake force, but a higher H will also increase the moment arm).
13. On the other hand, the presence of scour will reduce the depth of the foundation by y_{max}. This in turn will change the point of fixity of the column L_e as shown in Equation 10.
14. For the realizations of the time-dependent variables A and y_{max} and all the other time-independent variables, the moment applied on the bridge column is obtained from Equation 30.
15. The moment obtained from Step 14 gives the maximum moment expected to be applied during one flooding season due to the possible combination of earthquake forces and scour.
16. When the flooding season is over, and the scour hole is refilled, an earthquake might still occur and the applied moment for the earthquake that might hit during the dry season is calculated in the same manner described above, but without scour (i.e., with $y_{max} = 0.0$).
17. The higher of the two moments obtained from the dry season and the flooding season becomes the maximum yearly moment for the bridge.
18. Since there are 75 years within the design life of the bridge, the process starting with Step 4 is repeated 75 times. The maximum moment from all the 75 iterations will provide one realization of the maximum 75-year applied moment.
19. Steps 4 through 18 assumed that all the random variables, except for y_{max} and A, are set at values that were kept fixed over the design life of the bridge. These variables are Manning's number, n; the scour modeling factors λ_Q and λ_{sc}; the stream bed condition factor, K_3, as well as the earthquake modeling factor λ_{eq}; the spectral factor, C'; the period, T; the weight, W; and the response modification factor, R. The means, COVs and probability distributions of these variables that are sampled only once for the bridge design life are given in Tables 3 and 11. Failure of the bridge is verified by comparing the maximum 75-year applied moment to the moment capacity established in Step 3.
20. The Monte Carlo simulation is continued by repeating Steps 3 through 19 by first creating another set of realizations for the time-independent random variables, then calculating the maximum 75-year applied moment, and checking whether failure will occur. In the calculations presented in this appendix, the calculations are repeated a total of 100,000 times. The probability of failure is estimated as the ratio of the number of failures that are counted in Step 19 divided by the total number of iterations (100,000). The reliability index, β, is calculated from inverting the following equation:

$$P_f = \Phi(-\beta) \tag{34}$$

where P_f is the probability of failure and Φ is the cumulative normal distribution function.

21. The reliability calculations use the same safety margin given in Equation 31. This safety margin equation considers only the failure of the bridge column due to bending moment. Other failure modes such as failure in the soil due to the reduction of the soil depth have also been considered as will be discussed further below.

5.2 Results for Bending of Bridge Column

The reliability calculations are first executed for the five earthquake sites with the discharge data of the Cuyahoga River. The results illustrated in Figure 11 show that scour does not significantly affect the reliability index of the bridge for the column failure mode because as explained earlier, the presence of scour reduced the stiffness of the system, but at the same time increased the moment arm resulting in little change in the probability of failure of the column under bending loads. The presence of scour, however, would affect other failure modes, particularly the failure of the soil. This phenomenon is explained in Section 5.3.

5.3 Failure of Soil Due to the Combination of Scour and Earthquake Loads

The bridge could fail in different possible modes. These include moment failure at the base of the columns, shearing failures along the length of the columns, failure of the soil due to lateral loads, and so forth. The analysis performed above has shown that the presence of scour did not significantly affect the safety of the column for failure in bending. In this section, the failure of the foundation due to lateral forces is analyzed.

The model used assumes an equivalent static, linear-elastic behavior of the soil following Rankine's method as described by Poulos and Davis (1980). For the soil conditions of the site, the internal friction angle of the sand, ϕ, is equal to 35°. The buoyant unit weight of sand is 60 lb/ft^3. The free body diagram for the column-foundation-soil system is shown in Figure 12.

In Figure 12, F is the inertial force (equivalent applied force), H gives the effective height of the column to the point of fixity, and P_p is the passive resultant resisting force of the soil (produced by the triangular soil pressure resisting the motion). According to Poulos and Davis (1980), the active force P_p is given as follows:

$$P_p = \frac{3\gamma D K_p L^2}{2} \tag{34a}$$

where

γ = the specific weight of sand,
L = the depth of the pile;
D = the diameter of the pile, and
K_p = the Rankine coefficient, which is given by

$$K_p = \frac{1+\sin(\phi)}{1-\sin(\phi)} \tag{35}$$

where $\phi = 35°$ is the angle of friction for sand.

5.3.1 Definition of Failure

Failure of the soil due to lateral load may occur under two different cases: (1) no hinges form in the column and the soil is unable to resist the applied lateral force on top of the column and (2) a hinge forms in the column at the point of fixity and the soil is unable to resist the shearing forces transferred from the hinge. For Case 1, the applied lateral force is obtained from Equation 30a as

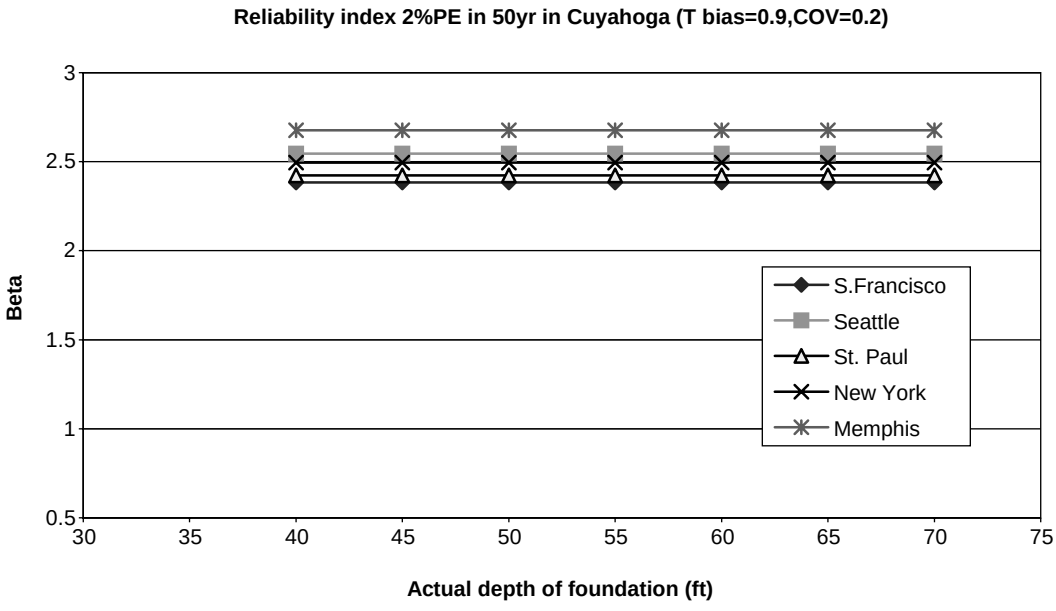

Figure 11. Effect of scour on the reliability index.

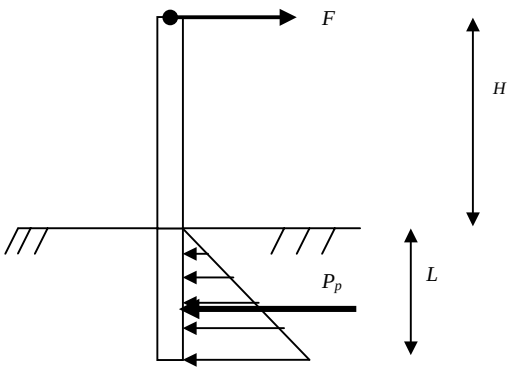

Figure 12. Free body diagram of bridge system.

$$P_{\text{appl}} = \lambda_{eq} C' S_a(t' T) * A * W. \tag{36}$$

Notice that the response modification factor is not used to calculate the applied lateral force on the system when no hinges are formed (i.e., when the column remains in the linear elastic range).

For Case 2, the applied force is

$$F_{\text{appl}} = \frac{M_u}{H} \tag{37}$$

where M_u is the ultimate moment capacity of the column. The actual ultimate moment capacity is a random variable with statistics related to the nominal capacity through a bias of 1.14 and a COV of 13%, as explained earlier. The safety margin for the failure of the soil is given as

$$Z = P_p - F_{\text{appl}} \tag{38}$$

where failure occurs if the safety margin Z is less than 0. P_p is the lateral force capacity of the soil. The presence of scour will lower the applied force of Equation 36 because it will reduce the stiffness of the system. Scour would increase the moment arm H, which would also lower the applied force calculated from Equation 37. On the other hand, scour will decrease the length of the foundation L, thus reducing the capacity of the foundation to resist the applied lateral loads. The fact that L is raised to the second power in Equation 34a indicates that the effect of the reduction of L on the foundation's capacity is significant.

Both P_p and F_{appl} of Equation 38 are random variables. Poulos and Davis (1980) mention that the bias observed in test results compared with Equation 34a is on the order of 1.50. In addition, the foundation's capacity to resist lateral load as calculated in Equation 34a is a function of the Rankine pressure coefficient, K_p, the unit weight of sand, γ, and the angle of friction, ϕ. These are random variables with COVs that may exceed 20%. In particular, Becker (1996) gives the following values for the COV for the soil parameters: for the unit weight of soil, $V_\gamma = 7\%$; $V_\phi = 13\%$ for the angle of friction of sand; and for the Rankine pressure coefficients, $V_K = 20\%$. In addition to the uncertainties associated with calculating the Rankine coefficients, the difference between the soil resistance under static loads and dynamic loads must be considered. To account for the dynamic effects on soils, Bea (1983) proposed to use a cyclic factor with a bias of 1.0 and a COV of 15%. In addition to these parameters, which are time-independent random variables, the foundation strength is a function of the dimension of the foundation. The dimensions are all assumed to be deterministic. The summary of the input data used to calculate the reliability of the column foundation to resist lateral load is provided in Table 12.

In addition to the random variables identified in Table 12, the random variables listed in Tables 3 and 11 are used in the Monte Carlo simulation that calculates the reliability of the bridge system subjected to the combination of scour and earthquake loads. The results for the failure of the soil for the San Francisco site are provided in Figure 13.

The results shown in Figure 13 illustrate the importance of the foundation depth on the reliability of the bridge system against soil failure due to lateral loads when the bridge is subjected to the combination of the scour and earthquake loads. The increase in the reliability index is dramatic because a change in the foundation depth from 50 ft to 60 ft produced a change in the reliability index from 2.14 to 3.05 for the case

TABLE 12 Input data for soil-related random variables

Variable	Mean Value	COV	Distribution Type
Unit weight of soil	60 lb/ft^3	7%	Normal
Angle of friction	35°	13%	Normal
Rankine earth pressure	1.5 nominal value	20%	Normal
Cyclic effects	1	15%	Normal

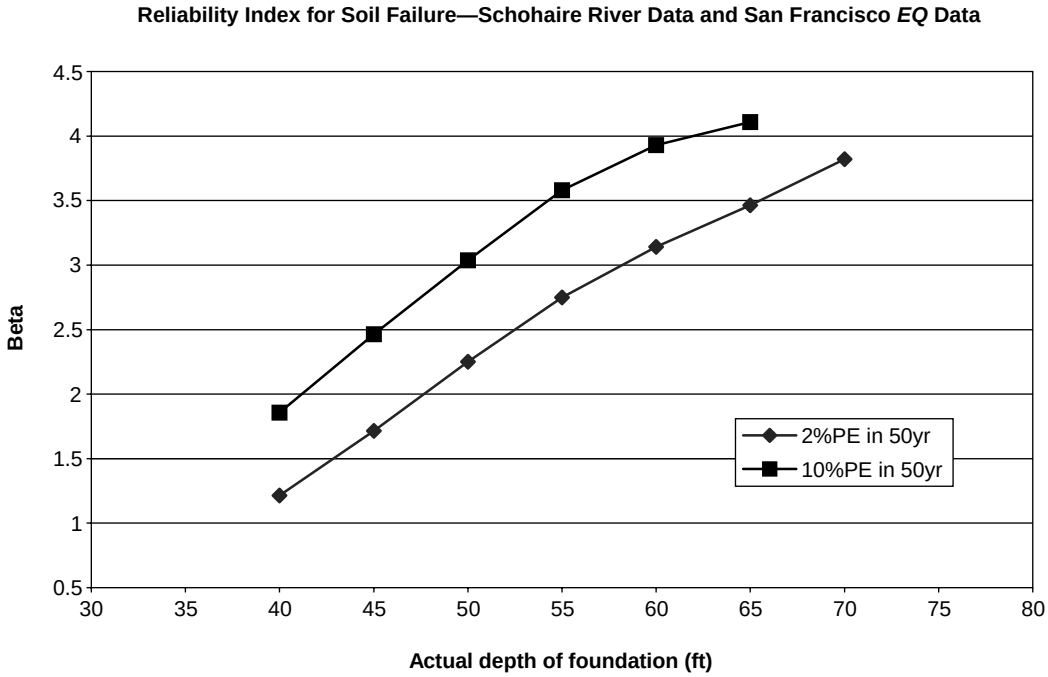

Figure 13. Reliability index for soil failure as a function of foundation depth.

when the bridge is designed such that the column capacity satisfies the NEHRP criteria for 2% probability of exceedance in 50 years. It is also noted that when the bridge columns are designed with weaker moment capacity, as is the case when the design is set to satisfy the earthquake level corresponding to 10% probability of exceedance in 50 years, the reliability index is higher than for 2% case because the columns will transmit a smaller force to the foundation as described by Equation 37. Of course, the lower capacity will mean a higher probability of column failure in bending.

To study the effect of scour on the reliability index for soil failure, the same case analyzed in Figure 13 for the San Francisco earthquake is repeated assuming that no scour could occur. The results are illustrated in Figure 14, which shows that the presence of scour would decrease the reliability index for soil failure by about 1.50 for the case when the foundation is 40-ft deep. The difference decreases to about 0.0 for very deep foundations of 70 ft. This is because the effect of scour on the capacity of the soil is minimal when the foundation is very deep. The results from Figure 14 can be used to calibrate the load factors for the combination of scour and earthquake loads as will be illustrated in Section 6.

6. CALIBRATION OF LOAD FACTORS FOR COMBINATION OF SCOUR AND EARTHQUAKE LOADS

The results obtained in the previous section can be used to calibrate the appropriate load factor for the combination of scour and earthquake loads. For example, as seen in Table 9, current design specifications would require that the foundation depth be equal to 43.7 ft (rounded up to 44 ft) if the bridge shown in Figure 1 of Section 1.1 were to be located in the San Francisco site. The 44-ft foundation depth would have produced a reliability index of 2.1 if scour were not considered. If the same target reliability index should be attained when scour is included, then the depth of the foundation should be 49 ft. This would require extending the foundation by another 5 ft. Notice that for the Schohaire River (used to model the occurrence of scour in Figure 14), the expected 100-year scour depth is 17.34 ft, as shown in Table 2. Hence, for the bridge to achieve the same target reliability index, it will not be necessary to extend the foundation by the 17.34 ft calculated from the scour alone; an extension of only 5 ft is sufficient. This smaller extension reflects the lower probability of having a high level of scour in combination with a high earthquake load. Also, one should note that the effects of earthquakes and scour are not linear. Hence, the interaction and the correlation between the two effects may require a reduction in the amount of scour considered when the analysis of the bridge for earthquake loads is performed.

It is also noted that if a target reliability index of 3.5 is to be achieved, the foundation depth should be extended to about 63 ft if no scour is to be considered, while the foundation should be about 65-ft deep for the combination of scour and earthquake loads. To satisfy a target reliability index of 2.5, the depth of the foundation for no scour should be 48 ft while 53 ft would be required to account for the combination of scour and earthquake loads. These results are summarized in Table 13. Clearly there are an infinite number of load factor combinations that would allow us to

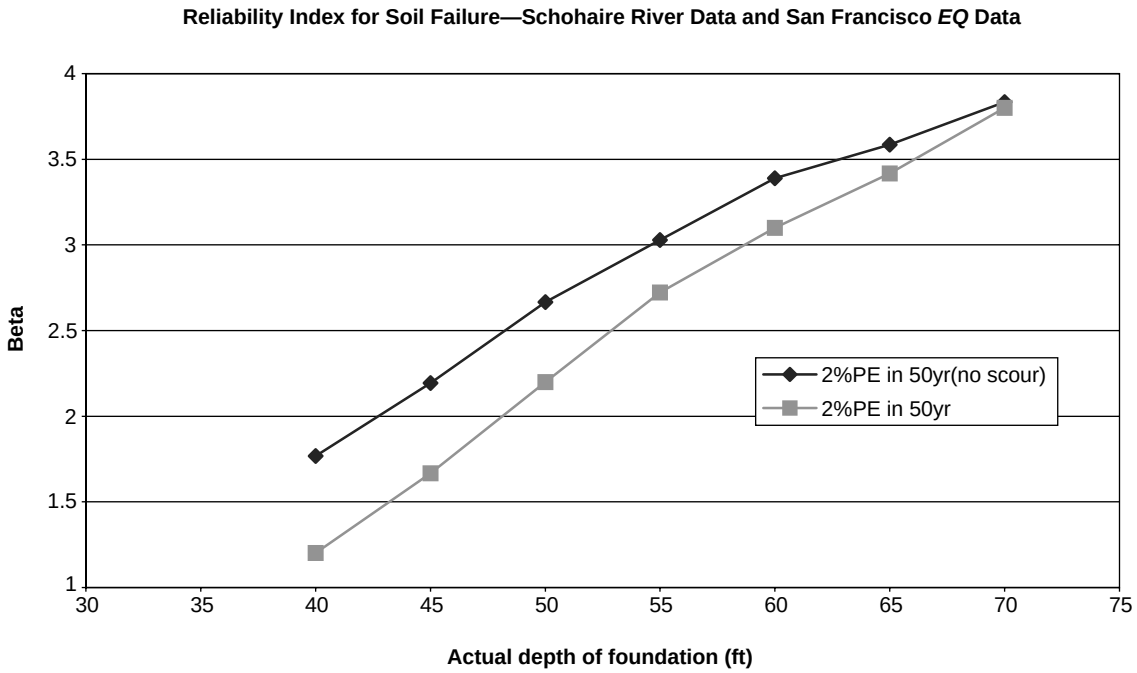

Figure 14. Comparison of reliability index for San Francisco site with scour and without scour.

TABLE 13 Required foundation depth to satisfy different reliability targets

Target reliability index	Depth for no scour	Depth for scour + *EQ*	Current *EQ* design requirement
1.5	37 ft	43 ft	44 ft
2	43 ft	48 ft	44 ft
2.5	48 ft	53 ft	44 ft
3	55 ft	58 ft	44 ft
3.5	63 ft	65 ft	44 ft

design the foundation to achieve the target reliability levels For example, to achieve the required foundation depth, one option would be to use a load factor on earthquake loads equal to 1.0 and to increment the foundation depth by a factor of 17.34-ft for design scour depth. For example, by taking the required 44 ft depth for earthquake alone with 0.52 times the design scour depth, a total foundation depth of 53 ft is achieved, leading to a reliability index of 2.5. The different load factors that may be used on scour to achieve different reliability targets are listed in the last column of Table 13. If a target reliability index of 2.0 is required, then a load factor on scour of 0.23 will be sufficient.

The results summarized in Table 13 are for illustration only as the data from the other sites and rivers are still being summarized and analyzed. However, it is noted that the differences from the different sites and rivers are expected to be minimal, as demonstrated in the previous sections, in which it was observed that the reliability indexes calculated using the models described in this report were similar for the different site locations and rivers considered.

REFERENCES FOR APPENDIX C

American Association of State Highway and Transportation Officials (1994). *AASHTO LRFD Bridge Design Specifications,* Washington, DC.

Applied Technology Council (1981). *Seismic Design Guidelines for Highway Bridges*, ATC-6, Redwood City, CA.

Bea, R.G. (1983). "Characterization of the Reliability of Offshore Piles Subjected to Axial Loadings," *Proceedings of the ASCE Structures Congress*, October 1983, TX.

Becker, D.E (1996). "18th Canadian Geotechnical Colloquium: Limit States Design for Foundations, Part II: Development for the National Building Code of Canada," *Canadian Geotechnical Journal,* Vol. 33; pp. 984–1007.

Briaud, J.L., Ting, F.C.K., Chen, H.C, Gudavalli, R., Perugu, S., and Wei, G. (1999). "SRICOS: Prediction of Scour Rate in Cohesive Soils at Bridge Piers," *ASCE Journal of Geotechnical and Environmental Engineering*, Vol. 125, No. 4 (April 1999); pp. 237–246.

Chopra, A.K., and Goel, R.K. (2000). "Building Period Formulas for Estimating Seismic Displacements," *EERI Earthquake Spectra*, Vol. 16, No. 2.

Ellingwood B., Galambos, T.V., MacGregor, J.G., and Comell, C.A. (1980). *Development of a Probability Based Load Criterion for American National Standard A58*, National Bureau of Standards, Washington, DC.

Frankel, A., Harmsen, S., Mueller, C., Barnhard, T., Leyendeker, E.V., Perkins, D., Hanson, S., Dickrnan, N., and Hopper, M. (1997). "USGS National Seismic Hazard Maps: Uniform Hazard Spectra, De-aggregation, and Uncertainty," *Proceedings of FHWA/ NCEER Workshop on the National Representation of Seismic Ground Motion for New and Existing Highway Facilities*, NCEER Technical Report 97-0010, SUNY Buffalo, NY; pp. 39–73.

Haviland, R. (1976). "A Study of Uncertainties in the Fundamental Translational Periods and Damping Values for Real Buildings," MIT reports, Cambridge, MA.

Hwang, H.H.M., Ushiba, H., and Shinozuka, M. (1988). "Reliability Analysis of Code-Designed Structures under Natural Hazards," Report to MCEER, SUNY Buffalo, NY.

Hydraulic Engineering Center (1986). "Accuracy of Computed Water Surface Profiles," U.S. Army Corps of Engineers, Davis, CA.

Johnson, P.A. (1995). "Comparison of Pier Scour Equations Using Field Data," *ASCE Journal of Hydraulic Engineering*, Vol. 121, No. 8; pp. 626–629.

Landers, M.N., and Mueller, D.S. (1996). "Channel Scour at Bridges in the United States," FHWA-RD-95-l84, Federal Highway Administration, Turner-Fairbank Highway Research Center, McLean, VA.

Liu, W.D., Ghosn, M., Moses, F., and Neuenhoffer, A. (2001). *NCHRP Report 458: Redundancy in Highway Bridge Substructures*, Transportation Research Board of the National Academies, Washington, DC.

Liu, D., Neuenhoffer, A., Chen, X., and Imbsen, R. (1998). "Draft Report on Derivation of Inelastic Design Spectrum," Report to NCEER, SUNY Buffalo, NY.

Miranda, E. (1997). "Strength Reduction Factors in Performance-Based Design," EERC-CUREe Symposium in Honor of Vitelmo V. Bertero, Berkeley, CA.

National Earthquake Hazards Reduction Program (1997). *Recommended Provisions for Seismic Regulations for New Buildings and Other Structures*, Federal Emergency Management Agency, FEMA 302, Building Safety Council, Washington, DC.

Newmark, N.M., and Hall, W.J. (1973). "Seismic Design Criteria for Nuclear Reactor Facilities," *Building Practices for Disaster Mitigation, Report No. 46*, National Bureau of Standards, U.S. Department of Commerce; pp. 209–236.

Nowak, A.S. (1999). *NCHRP Report 368: Calibration of LRFD Bridge Design Code*, Transportation Research Board of the National Academies, Washington, DC.

Poulos, H.G., and Davis, E.H. (1980). *Pile Foundation Analysis and Design*, Krieger Publishing Co., FL.

Priestley, M.J.N., and Park, R. (1987). "Strength and Ductility of Concrete Bridge Columns Under Seismic Loading," *ACI Structural Engineering Journal*, January–February.

Richardson, E.V., and Davis, S.R. (1995). *Evaluating Scour at Bridges*, 3rd edition. Report No. FHWA-IP- 90-0 17, Hydraulic Engineering Circular No. 18, Federal Highway Administration, Washington, DC.

Seed, H.B., Ugas, C., and Lysmer, J. (1976). "Site-Dependent Spectator Earthquake-Resistant Design," *Bulletin of the Seismological Society of America*, Vol. 66, No. 1 (February 1976); pp. 221–243.

Shirole, A.M., and Holt, R.C. (1991). "Planning for a Comprehensive Bridge Safety Assurance Program," *Transportation Research Record 1290*, Transportation Research Board of the National Academies, Washington, DC; pp. 39–50.

Stewart, J.P., Seed, R.B., and Fenves, G.L. (1999). "Seismic Soil Structure Interaction in Buildings, II: Empirical Findings." *ASCE Journal of Geotechnical and Geoenvironmental Engineering*, Vol. 125, No. 1.

Takada, T., Ghosn, M., and Shinozuka, M. (1989). "Response Modification Factors for Buildings and Bridges," *Proceedings from the 5th International Conference on Structural Safety and Reliability*, ICOSSAR 1989, San Francisco; pp. 415–422.

Zahn, F.A., Park, R., and Priestly, M.J.N. (1986). "Design of Reinforced Concrete Bridge Columns for Strength and Ductility," Report 86- 7, University of Canterbury, Christchurch, New Zealand.